January 2019

Vehicle Rollover Stability And Path Planning In Adas Using Model Predictive Control

Xinyue Zhang
Wayne State University, gl0998@wayne.edu

VEHICLE ROLLOVER STABILITY AND PATH PLANNING IN ADAS USING MODEL PREDICTIVE CONTROL

by

XINYUE ZHANG

THESIS

Submitted to the Graduate School

of Wayne State University,

Detroit, Michigan

in partial fulfillment of the requirements

for the degree of

MASTER OF SCIENCE

2019

MAJOR: ELECTRIC-DRIVE VEHICLE

ENGINEERING

Approved By:

_____

Advisor   Date

_____

Co-advisor   Date

ACKNOWLEDGEMENTS

TABLE OF CONTENTS

LIST OF FIGURES

LIST OF TABLES

CHAPTER 1 INTRODUCTION

Advanced Driver Assistance Systems (ADAS) have been developed in recent years to significantly improve safety in driving and assist driver's response in extreme situations in which quick decisions and maneuvers are required. Common features of ADAS in modern vehicles include automatic emergency braking (AEB), lane keeping assistance (LKA), electric stability control (ESC), and adaptive cruise control (ACC). While these features are developed primarily based on sensor fusion, image processing and vehicle kinematics, the importance of vehicle dynamics must not be overlooked to ensure that the vehicle can follow the desired trajectory without inducing any instability. In many extreme situations such as object avoidance, fast maneuvering of vehicles with high center of gravity might result in rollover instability, an event with a high fatality rate. It is thus necessary to incorporate vehicle dynamics into ADAS to improve the robustness of the system in the path planning to avoid collision with other vehicles or objects and prevent vehicle instability. The objectives of this thesis are to examine the efficacy of a vehicle dynamics model in ADAS to simulate rollover and to develop an active controller using Model Predictive Control (MPC) to manipulate the front-wheel steering and four-wheel differential braking forces, which are related to active steering as well as dynamic stability control for collision avoidance. The controller is designed using the model predictive control approach. A four degree-of-freedom vehicle model is simulated and tested in various scenarios. According to simulation results, the vehicle controller by the MPC controller can track the predicted path within error tolerance. The trajectories used in different simulation scenarios are generated by the MPC controller.

1.1 Motivation

Safety, comfort and economy are the three most important aspects when considering the design and manufacturing of a vehicle, especially safety. The safety of vehicles is affected by various factors including:

Environment: Road friction, traffic conditions, etc.

Driver: Distraction, response capability, driving skills, preference, etc.

Vehicle: Type of vehicles (center of gravity, suspension, steering, etc.), control systems

Usually, a human driver is in control when driving a car without any assistant systems. However, innumerable accidents happened because of drivers, who could be distracted and were not able to handle sudden or extreme situations. To address the above safety issues related to drivers, Advance Driver Assistance Systems (ADAS) have been proposed and become more and more popular when fully autonomous driving can hard be achieved immediately. ADAS means some automated features are introduced, such as automatic emergency braking (AEB), lane keeping assistance (LKA), electric stability control (ESC), adaptive cruise control (ACC), etc. ADAS features/functions have gradually become standard on different models of cars to attract customers [1]. It is a common sense that ADAS consist of pre-crash active systems, helping drivers to avoid collision. Image a case that the subject vehicle is following a preceding vehicle while suddenly the preceding vehicle changes to another lane without deceleration because the vehicle before the preceding vehicle stops. It will impede the ability of the ADAS systems to detect the obstacle so that it would be hard for the ego vehicle to stop safely. Thus, there must be a decision-making system to have the subject vehicle move to another direction. It's better

to execute appropriate ADAS functions according to different situations.

Rollover in extreme situations is an unsolved problem with a high fatality rate. Compared to common passenger vehicles, it is more necessary for trucks and buses have a higher center of gravity to be equipped with certain ADAS features because the long daily routine driving hours greatly impact the driving capability and attention of those drivers (such as truck drivers and long-distance tourist bus drivers). Moreover, the stability performance is equally important to collision avoidance, especially in fast maneuvers, while a severe problem related to stability is rollover. In this aspect, vehicles with a high center of gravity have a much greater risk of rollover than common passenger vehicles. There are over 500 large truck rollover accidents that occur each year throughout the U.S. according to the National Highway Traffic Safety Administration [2]. Over 60 percent of these rollover accidents result in fatalities [2]. According to current literatures [3,4,30,31], real-time rollover prevention system has been researched as a popular topic. Rollover prevention can be grouped into two categories: rollover warning system by using prediction algorithms, and active roll control [3]. As shown in Figure 1, for active roll control, there are five main directions: four-wheel steering, differential braking, active roll-bar, in-wheel motor [4], and active suspension. The first two ways are used to prevent rollover by controlling yaw motion while the latter three ways are achieved by controlling roll motions. This thesis aims to develop an active controller to control front-wheel steering and differential braking forces of vehicles to prevent rollover as well as collision, which can be classified to active steering system (ASS) as well as dynamic stability control (DSC) used for collision avoidance.
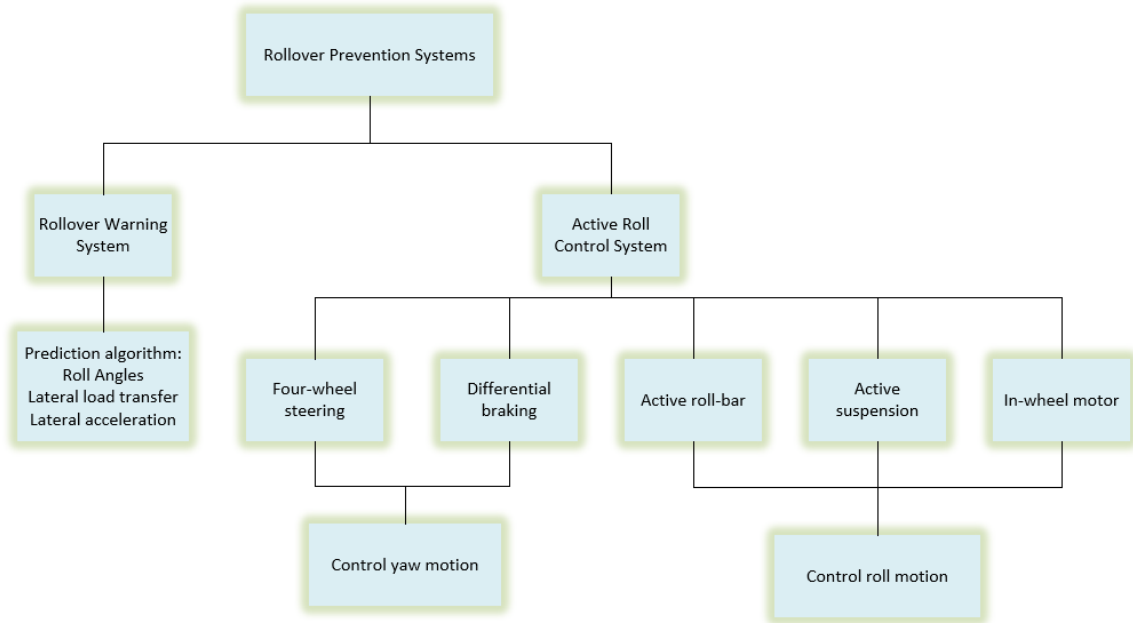
Figure 1. Rollover Prevention Systems Architecture Diagram.

1.2 Overview of ADAS System

The entire ADAS system includes three fundamental aspects: perception, vehicle dynamics and control. Thus, the research activities on active rollover prevention control can be divided into three aspects, as summarized in Table 1.

This thesis will not work on sensor fusion or any ADAS algorithm development. Rather, it will focus on the vehicle dynamics modeling and controller design as well as the combination of sensor inputs and controlling for rollover prevention.

Table 1. Three aspects of ADAS and their associated problems and directions

Aspects	Contents	Function	Tools
ADAS algorithms development	Computer vision algorithms Support Vector Machine (SVM), Histogram of Oriented Gradients (HOG) and Birds-Eye view	Used for vehicle detection and lane detection	Camera
	Kalman Filter, etc.	Used to track the surrounding vehicles' position and velocity with noisy lidar and radar measurements	Lidar&/ radar
Vehicle dynamics analysis	Appropriate model	Used to obtain differential equations subject to non-rollover and other physical constraints	N/A
MPC controller design	Prediction of future events and taking control actions accordingly [24]	Used for keeping the subject vehicle on the planned path (track) by adjusting the steering angle and braking (throttle)	MATLAB SIMULINK

1.3   Literature Review

All types of vehicles can roll over to some extent. However, vehicles having a higher center of gravity such as SUVs, pickups, buses and trucks are more susceptible to roll over if involved in a single-vehicle crash. NHSTA data show that nearly 85% of all rollover-related fatalities are the result of single-vehicle crashes [2]. The majority of rollover crashes and fatalities do not involve any other vehicle besides the one that rolled over and indicates that the driver behavior plays a significant role in rollover crashes [5]. Besides, rollover is one of the most common single accidents for heavy trucks, especially in the US, and for long-distance tourist buses mostly in developing countries. Thus, a reliable rollover prevention system is more than important to help drivers in decision making under extreme or emergent situations.

The rollover problem is mainly related to lane change, turning on a curvy road, and emergency braking [5]. There are several studies that develop algorithms or design controllers to improve the safety when the driver intends to change lane but are not clearly aware of rollover risk. Mahdi et al. proposed an algorithm, which combines the camera, inertial navigation sensor, and GPS data with the vehicle dynamics to estimate the vehicle path and the lane departure time. The lane path and vehicle path are estimated by using Kalman filters [6]. But they took the simplest geometric model and ideal situation for estimation. A geometric model is also called a kinematic model. The model does not either consider the slip angle which cannot be neglected for a moving car [7]. Therefore, it is necessary to develop a vehicle dynamic model considering steering angle, wheel rotation, yaw angle, roll angle, slip angle, etc. After building a vehicle dynamic model, the ego

vehicle status can be obtained while the environment status is achieved through sensors. A robust controller should respond quickly to the emergent and extreme situations by generating a best trajectory and controlling the vehicle to the expected trajectory.

Model predictive control (MPC), which is also called receding horizon control, is very popular and frequently used in the industry for optimal control of multivariable systems with constrains [8]. Receding horizon means updating predictions and making decisions by using the most recent target and measurement data. It has been proven to achieve improved performance compared to conventional techniques. MPC can be divided into linear MPC (LMPC) and nonlinear MPC (NMPC). There are no absolutely pros and cons to each which kind of MPC but depending on whether the system is linear or nonlinear, and whether it is able to or at least easily to be linearized. It is usually understood that an MPC controller takes the place of the driver to make decisions using the observed sensory information, which has been already fused together. An MPC controller can correct driver's inputs to achieve the desired motions.

Many researchers have paid attentions to the design of a controller for motion planning, but they mostly only consider a kinematic model [9]. Very limited research has been done on considering vehicle dynamics for rollover prevention and motion planning using MPC simultaneously since the system is rather complicated because not only lateral dynamics but also longitudinal dynamics and roll motion need to be considered. It is noted that the motion planning consists of path planning and path tracking / following. Both can be implemented by an appropriate MPC controller. Usually LMPC is utilized in the path planning stage for simplification and efficiency while both LMPC and NMPC can be

utilized in the path following stage. A sample based MPC proposed by Caldwell et al. for an autonomous underwater vehicle can do real-time motion planning that uses a nonlinear vehicle model [10]. It incorporates Rapidly-exploring Random Tree (RRTs), Probabilistic Road Maps (PRM), which was also researched by Liu et al [11].

Actually, path planning is the first step ahead of path following. In other words, if we simulate a system by path following, the path is usually preset by humans, not generated by the system itself. We then compare and check how well the real path matches the planned one. Basically, designing a path planning controller is more difficult than that of path following. It is also a common way to verify a controller of tracking ability first before combining that with the path planning. Isaac Gwayi and Mohohlo S. Tsoeu discussed rollover prevention and path following of autonomous vehicle using nonlinear model predictive control [12]. The authors focused on the path following while the controller needs to have the planned trajectory first, then it controls the vehicle to follow the trajectory to the planned one. There are still many limitations as the MPC was used for cornering only, while many case scenarios, especially fast maneuvers, were not included. Moreover, the inputs to the controller are the driving torque and steering wheels without considering the braking situations.

Thomas et al. claimed that the coordination of the active control action with the driver's is a challenging Human-In-The-Loop (HIL) problem [13]. To allow us to focus on integrating vehicle dynamics into ADAS during extreme maneuvers, the driver's response or input is not taken into consideration. In this thesis, the system designed still has features of ADAS, or autonomous driving. Another innovation of this thesis is that two variables,

steering and velocity, are controlled under extreme situations so that the vehicle can switch from one ADAS function to another function according to different conditions. For example, when the vehicle encounters an obstacle ahead during ACC mode, it can automatically change to AEB or Lane Change mode, in which case, it can avoid collisions. This thesis will mainly focus on the vehicle model building and controller design. Chapter 2 will discuss typical scenarios encountered in extreme situations. Chapter 3 will develop a nonlinear model of vehicle dynamics. Chapter 4 will design a nonlinear model predictive control controller. The conclusion is then drawn in Chapter 5.

CHAPTER 2 SCENARIO ANALYSIS

Reasons for rollover accidents can vary with different situations. A detailed analysis of the dynamics in a particular rollover situation is presented in [14]. In this thesis, only some basic and common scenarios are discussed, and they could be extended further if needed. PreScan is used for the entire environment construction and sensors implementation so that its outputs can be directly used, including the ego vehicle position from GPS, the relative velocity and relative distance between the ego vehicle and the preceding vehicle from Radar. Usually, there are two approaches to avoid collisions when a car encounters an obstacle on highway: one is by automatic emergency braking activation (AEB), which applies up to two thirds of the braking power of the vehicle without a driver's intervention; the other is by changing to another lane along a safe trajectory. The condition for the vehicle to choose one method over the other is determined by difference between the relative distance and a calculated safe distance. As all of the scenarios are under unusual situations, meaning that radar and other sensors are impossible to detect the obstacle beforehand, and the AEB is relatively ineffective because there is not enough distance and time for the vehicle to stop safely without any collision. Hence, more in deepth research on rollover prevention is needed for sudden lane changing.

Highway traffic and safety engineers have already developed general standards for vehicle stopping distance and time [32]. If a road surface is dry, a light truck can safely reduce its speed with reasonably good tires at a rate of 15 ft/s^2. A good controller system can perform as well as a skilled driver who can significantly reduce the stopping distance and time, and the deceleration rate could exceed 20 ft/s^2. The table below shows the braking

distances regarding to different initial velocities.

Table 2. Braking / Stopping Distance

MPH	Ft./Sec.	Braking Deceleration Distance		Perception Reaction Distance		Total Stopping Distance	
55	80.7	144 feet	43.9 m	8.1 feet	2.5 m	152.1 feet	46.4 m
60	88	172 feet	52.5 m	8.8 feet	2.7 m	180.8 feet	55.1 m
65	95.3	202 feet	61.6 m	9.6 feet	3.0 m	211.6 feet	64.5 m
70	102.7	234 feet	71.3 m	10.3 feet	3.2 m	244.3 feet	74.5 m
75	110	268 feet	81.7 m	11 feet	3.4 m	279 feet	85.1 m
80	117.3	305 feet	93.0 m	11.8 feet	3.6 m	316.8 feet	96.6 m

It is noted that trucks need more time and longer distance to stop fully than common cars.

Described below are four common scenarios that we will consider in the simulation. The first three cases vary by increasing the number of lanes and number of vehicles occupying the lanes.

Case 1. Sudden stop of the leading vehicle in the original lane
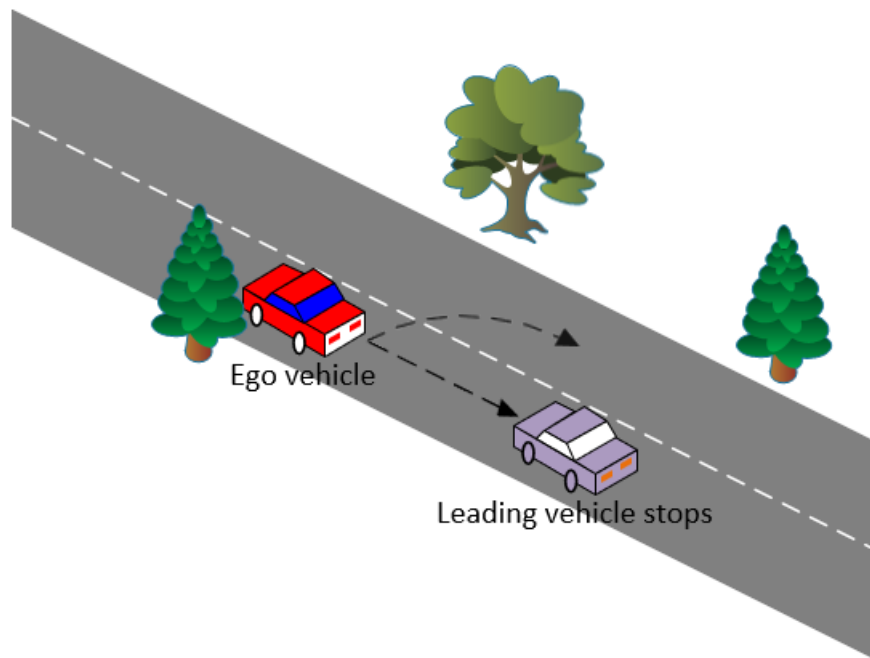
Figure 2. Case 1: Leading vehicle in the original lane stops suddenly

There are two possible ways for the ego vehicle to avoid a rear crash in this case: either stop straightforward or change lane to avoid the preceding vehicle if the ego vehicle cannot stop safely. For example, if the distance that the sensor detects the preceding car is smaller than 64.5 meters when the speed is 104 kph and above, it is impossible for the ego vehicle to stop safely even using the AEB (see Table 2. Braking / Stopping Distance). Thus, the only choice is to change to another lane, supposing that there are no other unexpected vehicles.

Case 2. Sudden stop of the Preceding vehicle in the initial lane plus vehicles in the adjacent lane.

There are also two possible approaches for the ego vehicle to make a decision in this case: either stop straightforward or change lane to avoid the preceding vehicle if the ego

vehicle cannot stop safely. However, the difference from case 1 is that the system needs to plan a best path to avoid the collision with the vehicle in the adjacent lane. Thus, not only the relative distance and velocity between the ego car and the preceding car are important, but also the relative distance and velocity between the ego car and the car in adjacent lane. All these factors impact the path / trajectory planning. The challenge of case 2 is that it requires more powerful sensors and computation ability of systems.
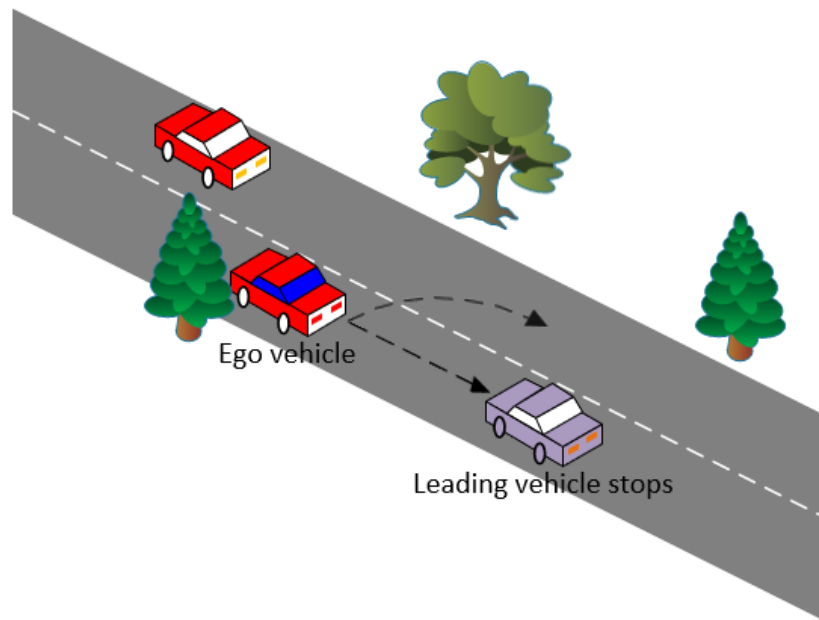
Figure 3. Case 2: Preceding vehicle in the initial lane stops suddenly plus vehicles in

adjacent lane

Case 3. More complicated scenario
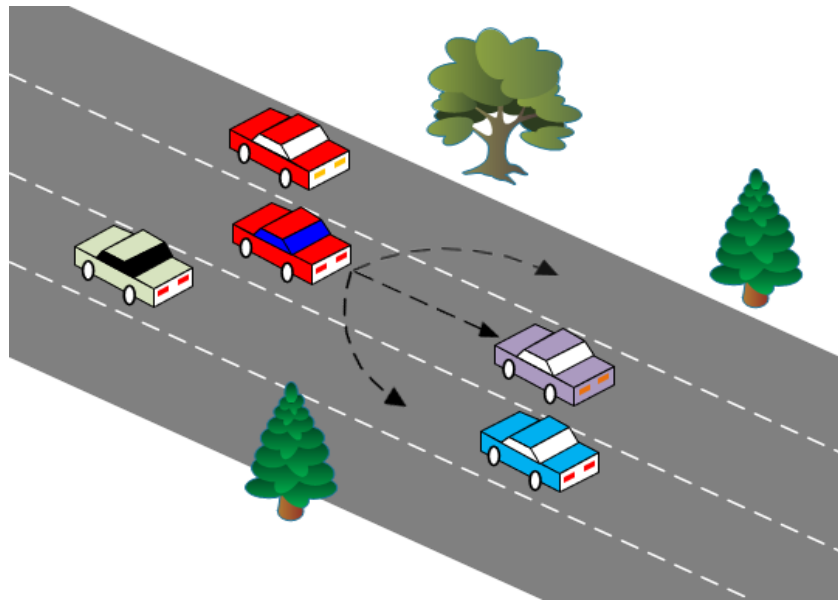
Figure 4. Case 3: Multiple obstacles scenario

Case 3 is the most complicated situation among the first three cases, because more inputs from the environment should be considered and detected, which requires a more robust algorithm and more powerful hardware that could handle varying parameters in the environment and assist the vehicle to make a proper decision. In Figure 4, there are three possible ways for the ego vehicle to avoid collision as well as rollover. The difficulty is that it may take more time for the system to process inputs and the situation is varying all the time. If the system is not robust enough, a wrong and dangerous decision can be made. There are other possible scenarios, for example, there is no possible path planning that could prevent rollover and collision at the same time. Under these situations, a trade-off between rollover and collision avoidance has to be made. Many researchers have focused on unavoidable collisions and worked on how to reduce the risk. However, it is still a major research. Thus, it will not be discussed in this thesis. All the cases discussed can be built in PreScan by adding trajectory, actuators, and sensors.

CHAPTER 3 MODELING OF VEHICLE DYNAMICS

A vehicle model as a rigid body has six degree-of-freedom (DOF), i.e., motions in three translational directions and three rotational directions. The translational motions are longitudinal, lateral and vertical motions, and the rotational motions are roll, pitch and yaw motions. Each motion represents a DOF. However, the rigid body model is too simplistic and does not account for the modeling of suspension, tires and other lumped mass units of the vehicle. On the other hand, it is not cost-effective to model every single aspect of the vehicle. Modelling a comprehensive vehicle model could also lead to high nonlinearity. Thus, different degrees of freedom of vehicle dynamic models have been developed for different purposes. In the rollover prevention problem, the wheels should be treated separately different from the chassis body. The lumped mass of body is the "sprung mass", and the wheels are denoted as "unsprung masses" [15]. Moreover, pitch and vertical motions can be neglected since they are less important in this research.

Similar to typical passenger cars, most buses have two axles, while each axle has one or more pairs of wheels. However, some heavy trucks have several different numbers of axles, varying with two to six or more axles. Since the center of gravity of heavy trucks are usually higher than passenger vehicles, there is higher possibility that it will rollover. Therefore, height of center of gravity is a significant factor that leads a heavy truck to roll over. Higher center of gravity has greater significance in causing the vehicle to rollover than the number of axles. In this research, we will take a two-axle, four-tire, single-unit truck as the research subject, which can make the results more general. The model can be further extended and applied to SUVs and buses with high center of gravity. Moreover, there is no difference

between a two-axle truck and a passenger car in the overall analysis. In Figure 5, a two-axle, four-tire, single-unit truck and its trailer is shown as,
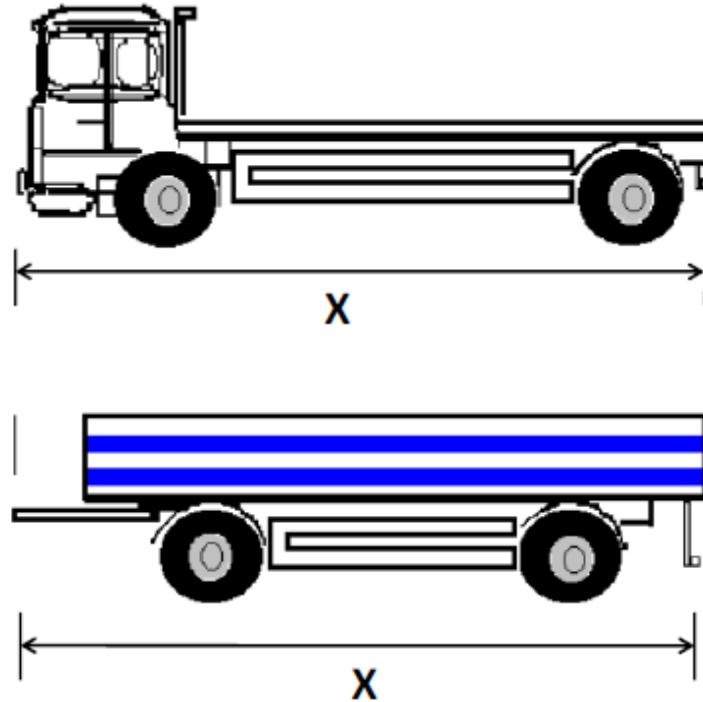
Figure 5. Two-axle, four-tire, single-unit truck and its trailer

3.1 Vehicle Coordinate Systems

To describe the motion of the vehicle, it is necessary to select an appropriate coordinate system for derivation of the equation of motion. A moving body can be treated as a reference frame that constantly provide reference coordinate for the observation of motion. Sprung mass and unsprung mass can be considered as coordinate system 1 and coordinate system 2, respectively. Coordinate system 1 is also called the body-fixed coordinate, as the starting point is fixed in the center of gravity of vehicle. It is noted that the mass of vehicle is concentrated in the sprung mass. The space-fixed coordinate X-Y-Z is used here as a reference frame. The space-fixed coordinate, X-Y-Z, is a rectangular Cartesian coordinate,

which follows right-hand rule, hence is usually defined as inertial coordinate system.
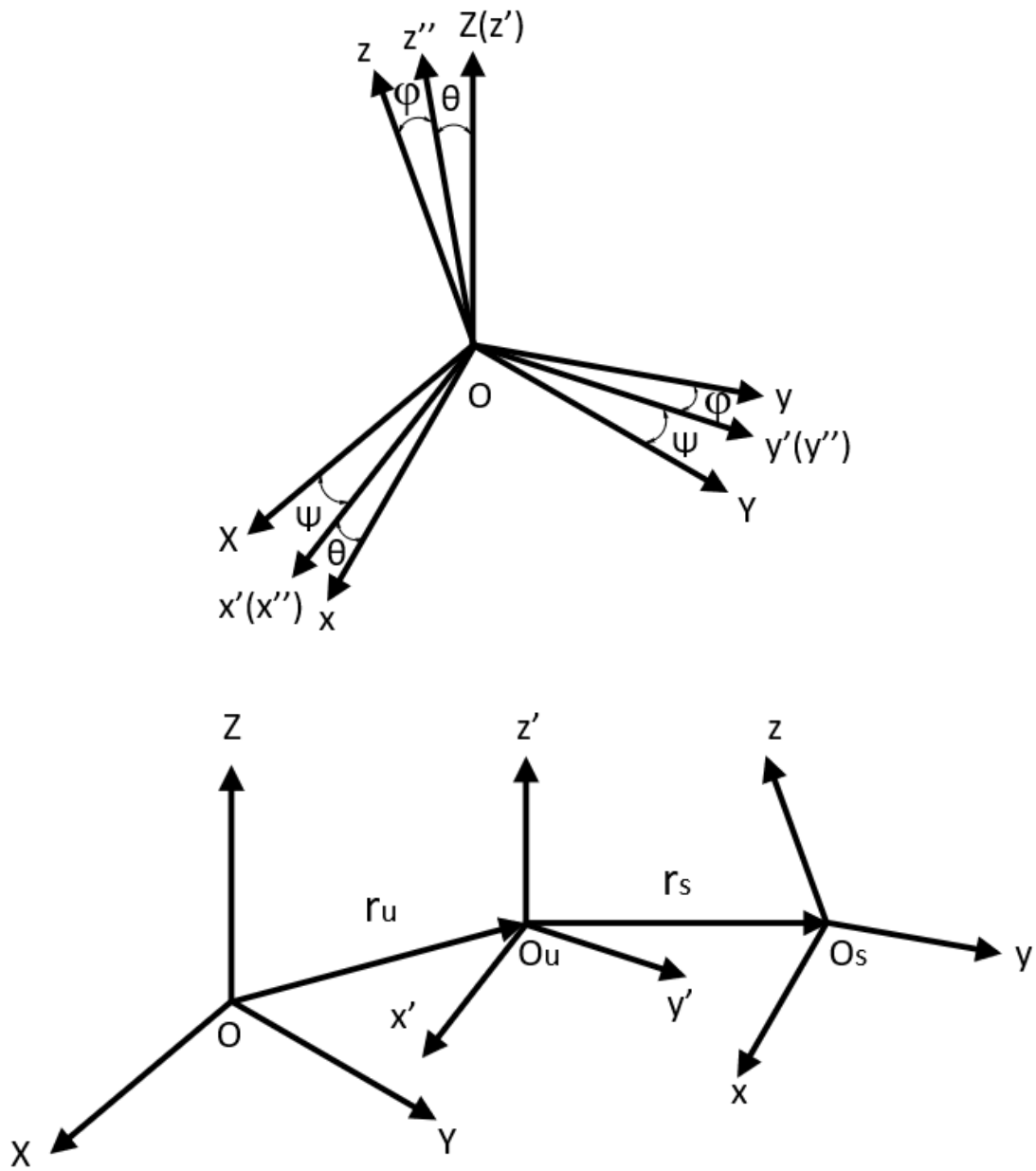
Figure 6. The relationships of three coordinate systems

X-Y-Z: inertial coordinate system;

x-y-z: body-fixed coordinate system (coordinate system 1);

x'-y'-z': unsprung mass coordinate system (coordinate system 2).

φ: roll angle; θ: pitch angle; Ψ: yaw angle. r_u and r_s stand for the position of unsprung mass with respect to the unsprung mass coordinate system, and the position of sprung mass with respect to the body-fixed coordinate system, respectively.

The unsprung mass coordinate system is obtained by rotating the inertial coordinate system through the yaw angle Ψ. The body-fixed coordinate system is obtained by 1) rotating the inertial coordinate system through the yaw angle Ψ, then 2) rotating the pitch angle θ, and finally 3) rotating the roll angle φ. In other words, the body-fixed coordinate system is obtained by rotating the unsprung mass coordinate system through the pitch angle θ then the roll angle φ.

3.2 Vehicle Chassis Model

The vehicle chassis model contains the sprung mass and the unsprung mass, as mentioned before. The vehicle chassis model has lateral, longitudinal, yaw and roll motions after ignoring the pitch rotational motion and vertical translational motion. Therefore, we can consider the chassis as a four-degree-of-freedom model as presented below.

Figure 7 shows a top view of the vehicle in the inertial frame, presenting the lateral, longitudinal, and yaw motions. $F_{yrl}, F_{yrr}, F_{yfl}, F_{yfr}$ denote the lateral forces of left rear wheel, right rear wheel, left front wheel and right front wheel, respectively. $F_{xrl}, F_{xrr}, F_{xfl}, F_{xfr}$ stand for the longitudinal forces of left rear wheel, right rear wheel, left front wheel and right front wheel, respectively.
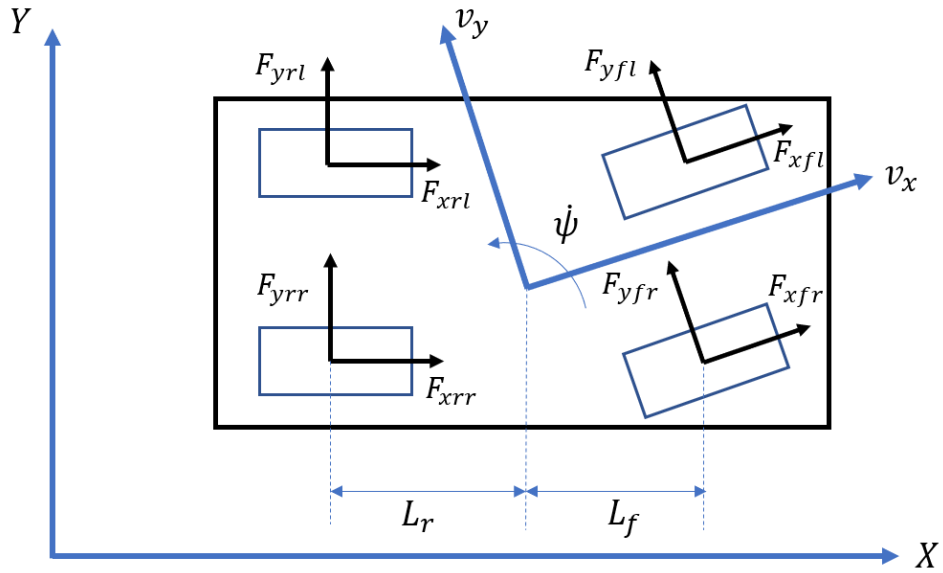
Figure 7. Top view of the vehicle chassis model

Since the coordinate system 2 is obtained by rotating inertial coordinate system through yaw angle, the angular velocities of unsprung mass and sprung mass with respect to the inertial coordinate system XYZ are,

$$[\omega_{O_u}] = \begin{Bmatrix} 0 \\ 0 \\ \dot{\psi} \end{Bmatrix}, [\omega_{O_s}] = \begin{Bmatrix} \dot{\varphi} \\ 0 \\ \dot{\psi} \end{Bmatrix} \qquad 3.1$$

While the translational velocities of unsprung mass can be represented under the coordinate system 2 with vertical velocity along the z-axis neglected,

$$[\dot{r}_u] = \begin{Bmatrix} v_x \\ v_y \\ 0 \end{Bmatrix} \qquad 3.2$$

Figure 8 shows a rear view of the vehicle, presenting the roll motion. F_{zl}, F_{zr} the vertical forces of left wheels and right wheels. δ denotes the steering angle of front wheels. Assume the steering angles of front wheels are same. $\dot{\Psi}$ the yaw rate [rad/s], φ the roll angle [rad].

v_x and v_y are the longitudinal and lateral velocities of the unsprung mass with respect to coordinate system 2. The velocity of unsprung mass can easily be measured compared with sprung mass. RC the roll center along the centerline of the track at the ground level. CG the center of gravity. m_s the sprung mass, the whole vehicle mass as well. H_{CG} the original height of center of gravity, h the actual height of center of gravity; L_r, L_f denote the distances of rear and front wheels from center of gravity, L_w is the vehicle width.
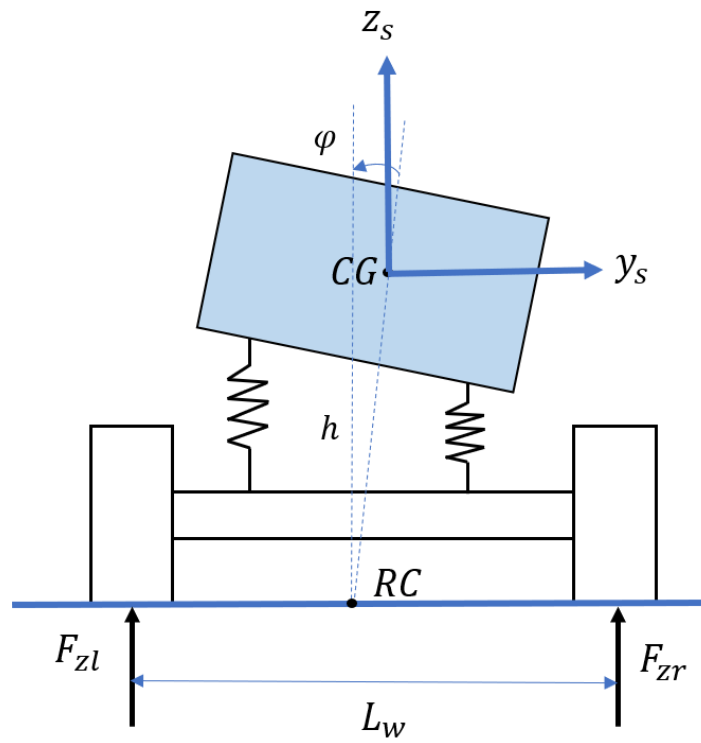
Figure 8. Rear view of the vehicle chassis model

The acceleration of the unsprung mass is,

$$[\ddot{r}_u] = \frac{D[\dot{r}_u]}{Dt} = \frac{d[\dot{r}_u]}{dt} + [\omega_{O_u}] \times [\dot{r}_u]$$

3.3

The first term on the right side of Eq. 3.3 is the partial derivative of time respect to the unsprung coordinate system,

$$\frac{d[\dot{r}_u]}{dt} = [\dot{v}_x \quad \dot{v}_y \quad 0]^T \tag{3.4}$$

The second term on the right side of Eq. 3.3 is the cross-product of the angular velocity and the longitudinal velocity, representing the rotation of the unsprung mass with respect to the space-fixed coordinate system,

$$[\omega_{O_u}] \times [\dot{r}_u] = \begin{vmatrix} i & j & k \\ 0 & 0 & \dot{\psi} \\ v_x & v_y & 0 \end{vmatrix}^T = [-v_y\dot{\psi} \quad v_x\dot{\psi} \quad 0]^T \tag{3.5}$$

Subtracting Eq. 3.4 and 3.5 into Eq. 3.3 leads to the following result,

$$[\ddot{r}_u] = [\dot{v}_x - v_y\dot{\psi} \quad \dot{v}_y + v_x\dot{\psi} \quad 0]^T \tag{3.6}$$

After getting the position, velocity and acceleration of the unsprung mass, those of the sprung mass can be presented in coordinate system 2,

$$[r_{s/u}] = \{0 \quad H_{CG} \sin\varphi \quad 0\}^T \tag{3.7}$$

The velocity of the sprung mass is

$$[\dot{r}_{s/u}] = \frac{D[r_{s/u}]}{Dt} = \frac{d[r_{s/u}]}{dt} + [\omega_{O_u}] \times [r_{s/u}] \tag{3.8}$$

The first term on the right side of Eq. 3.8 is the partial derivative of time with respect to the unsprung coordinate system,

$$\frac{d[r_{s/u}]}{dt} = [0 \quad \dot{\varphi}H_{CG}\cos\varphi \quad 0] \tag{3.9}$$

The second term on the right side of Eq. 3.8 is the cross-product of angular velocity and longitudinal velocity, representing the rotation of the sprung mass with respect to the unsprung coordinate system,

$$[\omega_{O_u}] \times [r_{s/u}] = \begin{vmatrix} i & j & k \\ 0 & 0 & \dot{\psi} \\ 0 & H_{CG}\sin\varphi & H_{CG}\cos\varphi \end{vmatrix}^T = [-H_{CG}\sin\varphi\,\dot{\psi} \quad 0 \quad 0]^T \qquad 3.10$$

Subtracting Eq. 3.9 and 3.10 into Eq. 3.8 leads to the following result,

$$[\dot{r}_{s/u}] = \{-H_{CG}\sin\varphi\,\dot{\psi} \quad \dot{\varphi}H_{CG}\cos\varphi \quad 0\}^T \qquad 3.11$$

To further get the acceleration of sprung mass,

$$[\ddot{r}_{s/u}] = \frac{D[\dot{r}_{s/u}]}{Dt} = \frac{d[\dot{r}_{s/u}]}{dt} + [\omega_{O_u}] \times [\dot{r}_{s/u}] \qquad 3.12$$

$$\frac{d[\dot{r}_{s/u}]}{dt} = [-H_{CG}\sin\varphi\,\ddot{\psi} - \dot{\varphi}H_{CG}\cos\varphi\,\dot{\psi} \quad \ddot{\varphi}H_{CG}\cos\varphi - \dot{\varphi}^2 H_{CG}\sin\varphi \quad 0]^T \qquad 3.13$$

$$[\omega_{O_u}] \times [\dot{r}_{s/u}] = [-\dot{\varphi}H_{CG}\cos\varphi\,\dot{\psi} \quad -H_{CG}\sin\varphi\,\dot{\psi}^2 \quad 0]^T \qquad 3.14$$

$$[\ddot{r}_{s/u}] \qquad 3.15$$

$$= [-H_{CG}\sin\varphi\,\ddot{\psi} - 2\dot{\varphi}H_{CG}\cos\varphi\,\dot{\psi} \quad \ddot{\varphi}H_{CG}\cos\varphi - \dot{\varphi}^2 H_{CG}\sin\varphi - H_{CG}\sin\varphi\,\dot{\psi}^2$$

Thus, the expression of the acceleration of the sprung mass with respect to the body-fixed coordinate system is,

$$[\ddot{r}_s] = [\ddot{r}_u] + \left[\ddot{r}_{\frac{s}{u}}\right] = \qquad 3.16$$

$$[\dot{v}_x - (v_y + 2\dot{\varphi}H_{CG}\cos\varphi)\dot{\psi} - H_{CG}\sin\varphi\,\ddot{\psi} \quad \dot{v}_y + v_x\dot{\psi} + H_{CG}(\ddot{\varphi}\cos\varphi - \dot{\varphi}^2\sin\varphi$$

Other than the translational force acting in the vehicle chassis, we can begin to consider rotational effects in our calculation, in other words, the angular acceleration. The angular moment of the sprung mass is

$$[H_s] = [I_u][\omega_{O_s}] \tag{3.17}$$

$$M = \dot{H}_s = \frac{d[I_u][\omega_{O_s}]}{dt} + [\omega_{O_u}] \times [I_u][\omega_{O_s}] \tag{3.18}$$

We can consider the moment of inertial of the sprung mass as,

$$[I_s] = \begin{bmatrix} I_{xx} & 0 & 0 \\ 0 & I_{yy} & 0 \\ 0 & 0 & I_{zz} \end{bmatrix}$$

I_{xx}: the roll inertial (kg m^2)

I_{yy}: the pitch inertial (kg m^2)

I_{zz}: the yaw inertial (kg m^2)

The body-fixed coordinate system is obtained from the rotating coordinate system through pitch angle and roll angle. The corresponding transformation matrices by a subscript that corresponds to the rotation axis is denoted as,

$$[R_x] = \begin{bmatrix} 1 & 0 & 0 \\ 0 & \cos\varphi & \sin\varphi \\ 0 & -\sin\varphi & \cos\varphi \end{bmatrix}$$

$$[R_y] = \begin{bmatrix} \cos\theta & 0 & -\sin\theta \\ 0 & 1 & 0 \\ \sin\theta & 0 & \cos\theta \end{bmatrix}$$

$$[R_z] = \begin{bmatrix} \cos\psi & \sin\psi & 0 \\ -\sin\psi & \cos\psi & 0 \\ 0 & 0 & 1 \end{bmatrix}$$

Only the roll motion participates the transformation from coordinate system 2 to body-fixed coordinate system. The formula of transformation of inertia can be obtained from fundamentals of vehicle dynamics [17]. Thus, the moment of inertia of unsprung mass is,

$$[I_s] = [R_x][I_u][R_x]^T$$

$$[I_u] = [R_x]^{-1}[I_s][[R_x]^T]^{-1}$$

3.19

$$[R_x]^{-1} = \begin{bmatrix} 1 & 0 & 0 \\ 0 & \cos\varphi & -\sin\varphi \\ 0 & \sin\varphi & \cos\varphi \end{bmatrix} = [R_x]^T$$

$$[[R_x]^T]^{-1} = \begin{bmatrix} 1 & 0 & 0 \\ 0 & \cos\varphi & \sin\varphi \\ 0 & -\sin\varphi & \cos\varphi \end{bmatrix} = R_x$$

$$[I_u] = [R_x]^T[I_s][R_x]$$

3.20

Subtracting Eq. 3.19 into Eq. 3.20 leads to the following result,

$$[I_u] = \begin{bmatrix} I_{xx} & 0 & 0 \\ 0 & \cos^2\varphi\, I_{yy} + \sin^2\varphi\, I_{zz} & \cos\varphi\sin\varphi\, I_{yy} - \sin\varphi\cos\varphi\, I_{zz} \\ 0 & \cos\varphi\sin\varphi\, I_{yy} - \sin\varphi\cos\varphi\, I_{zz} & \sin^2\varphi\, I_{yy} + \cos^2\varphi\, I_{zz} \end{bmatrix}$$

$$[I_u][\omega_{0_s}] = \begin{bmatrix} \dot\varphi I_{xx} \\ \dot\psi\,\cos\varphi\sin\varphi\,(I_{yy} - I_{zz}) \\ \dot\psi(\sin^2\varphi\, I_{yy} + \cos^2\varphi\, I_{zz}) \end{bmatrix}$$

Back to 3.18, the first term is,

$$\frac{d[I_u \omega_{O_s}]}{dt}$$

$$= \begin{bmatrix} \ddot{\varphi} I_{xx} \\ \ddot{\psi} \cos\varphi \sin\varphi \left(I_{yy} - I_{zz}\right) + \dot{\psi}\,\dot{\varphi}\left(I_{yy} - I_{zz}\right)(\cos^2\varphi - \sin^2\varphi) \\ \ddot{\psi}\left(\sin^2\varphi\, I_{yy} + \cos^2\varphi\, I_{zz}\right) + 2\dot{\varphi}\dot{\psi}(\cos\varphi\, I_{yy} - \sin\varphi\, I_{zz}) \end{bmatrix} \qquad 3.21$$

The second term is,

$$\left[\omega_{O_u}\right] \times \left[I_u \omega_{O_s}\right]$$

$$= \begin{vmatrix} i & j & k \\ 0 & 0 & \dot{\psi} \\ \dot{\varphi} I_{xx} & \dot{\psi}\cos\varphi\sin\varphi\,(I_{yy} - I_{zz}) & \dot{\psi}(\sin^2\varphi\, I_{yy} + \cos^2\varphi\, I_{zz}) \end{vmatrix}^T \qquad 3.22$$

$$= \begin{bmatrix} -\dot{\psi}^2 \cos\varphi \sin\varphi\,(I_{yy} - I_{zz}) \\ \dot{\psi}\dot{\varphi} I_{xx} \\ 0 \end{bmatrix}$$

Subtracting Eq. 3.21 and 3.22 into Eq. 3.18 leads to the following result,

$$M$$

$$= \begin{bmatrix} \ddot{\varphi} I_{xx} - \dot{\psi}^2 \cos\varphi \sin\varphi\,(I_{yy} - I_{zz}) \\ \ddot{\psi} \cos\varphi \sin\varphi \left(I_{yy} - I_{zz}\right) + \dot{\psi}\dot{\varphi}\left((\cos^2\varphi - \sin^2\varphi)(I_{yy} - I_{zz}) + I_{xx}\right) \\ \ddot{\psi}\left(\sin^2\varphi\, I_{yy} + \cos^2\varphi\, I_{zz}\right) + 2\dot{\psi}\dot{\varphi}(\cos\varphi\, I_{yy} - \sin\varphi\, I_{zz}) \end{bmatrix} \qquad 3.23$$

The equations discussed above are established in intrinsic coordinates. While not considering the external forces, the forces expressed in the equations are mainly generated in the contact surfaces between wheels and ground. Figure 7 has depicted the longitudinal and lateral forces of four tires. The total longitudinal and lateral forces are calculated as

$$F_x = F_{xrl} + F_{xrr} - (F_{yfl} + F_{yfr})\sin\delta + (F_{xfl} + F_{xfr})\cos\delta \qquad 3.24$$

$$F_y = F_{yrl} + F_{yrr} + \left(F_{yfl} + F_{yfr}\right)\cos\delta + (F_{xfl} + +F_{xfr})\sin\delta \qquad 3.25$$

The wheel load shifts because longitudinal acceleration and lateral acceleration vary. These forces distributed in each wheel can be calculated through the formula below, referring [18], F_{zfl}, F_{zfr}, F_{zrl}, F_{zrr} are normal forces acted on four wheels.

$$F_{zfl} = \frac{1}{2}m\left(\frac{L_r}{L}g - \frac{h}{L}a_x\right) - m\left(\frac{L_r}{L}g - \frac{h}{L}a_x\right)\frac{h}{L_w g}a_y$$

$$F_{zfr} = \frac{1}{2}m\left(\frac{L_r}{L}g - \frac{h}{L}a_x\right) + m\left(\frac{L_r}{L}g - \frac{h}{L}a_x\right)\frac{h}{L_w g}a_y$$

$$F_{zrl} = \frac{1}{2}m\left(\frac{L_f}{L}g + \frac{H_{CG}}{L}a_x\right) - m\left(\frac{L_f}{L}g + \frac{H_{CG}}{L}a_x\right)\frac{H_{CG}}{L_w g}a_y$$

$$F_{zrl} = \frac{1}{2}m\left(\frac{L_f}{L}g + \frac{H_{CG}}{L}a_x\right) + m\left(\frac{L_f}{L}g + \frac{H_{CG}}{L}a_x\right)\frac{H_{CG}}{L_w g}a_y$$

3.26

The rotational moments acting on the sprung mass in center of gravity over x-axis and z-axis are calculated as follows,

$$M_x = \frac{(F_{zfl} + F_{zrl})L_w}{2} - \frac{(F_{zfr} + F_{zrr})L_w}{2} + mgh\sin\varphi - M_s \qquad 3.27$$

$$M_z = (F_{yrl} + F_{yrr})L_r - [(F_{yfl} + F_{yfr})\cos\delta + (F_{xfl} + F_{xfr})\sin\delta]L_f$$

$$+ (F_{xrl} + F_{xfl}\cos\delta - F_{yfl}\sin\delta)\left(\frac{L_w}{2} + h\sin\varphi\right) \qquad 3.28$$

$$+ (F_{yrr}\sin\delta - F_{xfr}\cos\delta - F_{xrr})(\frac{L_w}{2} - h\sin\varphi)$$

In Eq. 3.27, M_s is the rotational moment generated by suspension, which will be mentioned in the suspension modeling section.

The next step is to establish equivalences between internal and external forces and rational moments, respectively. They are combined between Eq. 3.16 and 3.24 and 3.25,

3.23 and 3.27 and 3.28,

$$m \begin{bmatrix} \dot{v}_x - (v_y - 2\dot{\varphi}h\cos\varphi)\dot{\psi} - h\sin\varphi\,\ddot{\psi} \\ \dot{v}_y + v_x\dot{\psi} + h(\ddot{\varphi}\cos\varphi - \dot{\varphi}^2\sin\varphi - \sin\varphi\,\dot{\psi}^2) \\ 0 \end{bmatrix} = \begin{bmatrix} F_x \\ F_y \\ F_z \end{bmatrix} \qquad 3.29$$

$$M = \begin{bmatrix} \ddot{\varphi}I_{xx} - \dot{\psi}^2\cos\varphi\sin\varphi\left(I_{yy} - I_{zz}\right) \\ 0 \\ \ddot{\psi}\left(\sin^2\varphi\,I_{yy} + \cos^2\varphi\,I_{zz}\right) + 2\dot{\psi}\dot{\varphi}(\cos\varphi\,I_{yy} - \sin\varphi\,I_{zz}) \end{bmatrix}$$

$$3.30$$

$$= \begin{bmatrix} M_x \\ M_y \\ M_z \end{bmatrix}$$

Where M_y is neglected because the pitch motion is not considered.

Assume F_{zfl} is equal to F_{zrl}, and F_{zfr} is equal to F_{zrr}. Torque balanced equation for the unsprung mass about x axis is as follows,

$$\frac{F_{zr}L_w}{2} + M_s - \frac{F_{zl}L_w}{2} = 0 \qquad 3.31$$

Besides, the sum of normal forces is equal to vehicle gravity, then the normal forces can be simplified as,

$$F_{zfl} = F_{zrl} = \frac{M_s}{L_w} + \frac{mg}{2}$$

$$3.32$$

$$F_{zfr} = F_{zrr} = \frac{mg}{2} - \frac{M_s}{L_w}$$

3.3   Suspension Model

This vehicle model is modelled with a suspension. Compared with a rigid body vehicle model, it is more accurate to add a suspension model to the vehicle model when considering the roll motion of the vehicle. The roll motion can cause the movement of vehicle's center

of gravity, which can change the anti-rollover ability of the car's own weight. For a rigid model, the rollover threshold is given by,

$$\frac{a_y}{g} = \frac{L_w}{2h} + \beta \qquad\qquad 3.33$$

β is the ramp angle.

This equation explains why many curvy ramps have a degree of angle along with the x-axis. However, it neglects suspension and tire elasticity. In normal vehicles, the value of rollover threshold is relatively high, which may cause safety issues. Typically, more accurate suspension model brings more accurate results. In this research, a one-dimensional suspension model is used for computational concerns.

Each suspension system consists of a spring and a damper, which generates an anti-rotational moment over the x axis,

$$M_S = K\varphi + c\dot{\varphi} \qquad\qquad 3.34$$

In Eq. 3.34, K denotes spring constant of suspension system, c denotes damping constant of suspension system.

3.4 Tire model

Tire model is a very important part in vehicle dynamics modelling. Other than air resistance force, almost all external forces are generated in the contact surface between wheels and the ground. Researchers have developed various model for different purposes, such as the magic formula tire model, MF-SWIFT model, UnitTire model, FTire model family, and CDTire model family [19] The magic formula tire model is used as one of the most common tire models. Especially, the magic formula is widely used in the automotive

industry. The magic formula model contains various coefficients which must be acquired from the experimental data using curve fitting technique. In other words, these formulas are empirical formulas, which are relatively precise. The magic formula tire model is expressed as

$$y = D \sin[C \arctan\{Bx - E(Bx - E(Bx - \arctan Bx)\}] \qquad 3.35$$

Where, B = stiffness factor, C = shape factor, D = peak factor, E = curvature factor

In general, these four coefficients B, C, D, E are functions of the tire normal force F_z. Usually they are obtained through experiments, which vary under different road conditions.

The formula is usually used to calculate the tire longitudinal force, lateral force and aligning moment. In Eq. 3.35, the input x is the slip ratio λ or the slip angle α, corresponding to the output y - the tire longitudinal force F_x or lateral force F_y. Figure 9 [20] shows the relationship between tire slip angle and steering angle, as well as the actual moving direction of contact plane.
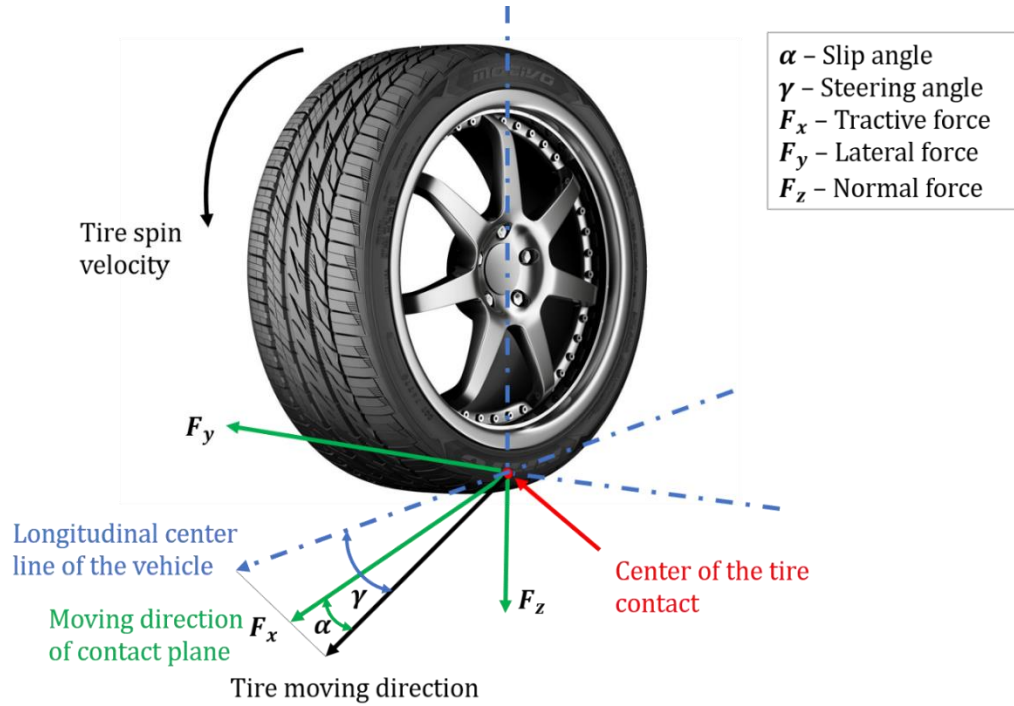
Figure 9. Tire slip angle and steering angle

The slip angles of front tires and rear tires are different, since the vehicle model is considered as front-wheel steering type. Vehicle kinemics is another reason. The longitudinal slip ratio λ and the slip angle α_f of front wheels and α_r of rear wheels are defined as,

$$\lambda = \begin{cases} \dfrac{R\omega - u}{R\omega} & R\omega > u \ during \ acceleration \\ \dfrac{R\omega - u}{u} & R\omega < u \ during \ braking \end{cases} \qquad 3.36$$

u denotes the axel longitudinal velocity, R denotes the radius of the wheel, ω denotes the rotating speed. The sign of slip ratio decides the direction of longitudinal forces.

$$\alpha_f = \delta - \frac{v_y + L_f \dot{\psi}}{v_x} \qquad\qquad 3.37$$

$$\alpha_r = \frac{-v_y + L_r \dot{\psi}}{v_x} \qquad\qquad 3.38$$

Due to ply steer, conicity and rolling resistance, the characteristics will be shifted in the horizontal and/or vertical directions [20]. Thus, some shifts should be included on the basis of general inputs,

$$x = x + S_H$$

$$y = y + S_V$$

$S_H = horizontal\ shift$

$S_V = vertical\ shift$

In this case, both longitudinal and lateral forces exist. In other words, it is a combined slip including sliding slip and longitudinal slip, which leads to a combined lateral-longitudinal tire model. However, the magic formula contains too many coefficients which must be acquired from the experiments. Another way to get the tire forces is by establishing a mathematical model for tires. Dugoff's tire model is another kind of versatile algorithms that are used to obtain tire forces [22]. Dugoff's model could provide calculation of forces regardless of combined lateral-longitudinal force generation. It is an alternative to the elastic foundation analytical tire model developed by Fiala (1954) for lateral force generation and by Pacejka and Sharp (1991) for combined lateral longitudinal and lateral forces generation. Then the longitudinal tire force of tire is given by,

$$\mathrm{F}_x = C_\lambda \frac{\lambda}{1+\lambda} f(\kappa)$$

3.39

The lateral tire force is given by,

$$\mathrm{F}_y = C_\alpha \frac{\tan \alpha}{1+\alpha} f(\kappa)$$

3.40

C_λ denotes the longitudinal tire stiffness and C_α denotes the lateral tire stiffness.

Where κ is given by,

$$\kappa = \frac{\mu F_z (1+\lambda)}{2\{(C_\lambda \lambda)^2 + (C_\alpha \tan \alpha)^2\}^{\frac{1}{2}}}$$

3.41

And

$$f(\kappa) = (2 - \kappa)\kappa \ \ if \ \kappa < 1$$

$$f(\kappa) = 1 \ \ if \ \kappa \geq 1$$

3.42

F_z denotes the vertical force on the tire. μ denotes the tire-road friction coefficient.

From [21], it is clear that in the case where the longitudinal slip ratio and lateral slip angle are small, κ is always bigger than 1, then longitudinal and lateral forces are expressed as below,

$$F_x = C_\lambda \frac{\lambda}{1+\lambda}$$

3.43

$$F_y = C_\alpha \frac{\alpha}{1+\alpha}$$

3.44

As mentioned in the chapter literature review, there are many roll-motion-control and yaw-motion-control based ways to prevent rollover. Most researches indicate that the rollover prevention feature can be included within stability control [22], basically focusing

on yaw motion. There are three typical types of stability control system that have been proposed and developed for yaw motion, 1) differential braking, 2) steer-by-wire, and 3) active torque distribution. Each proposed control system attracts attention from researchers in this order. Actually, the common feature of three systems is that they only have one manipulated variable/input, while the system I want to develop is able to control two variables simultaneously and the controller has fast response. Therefore, I combine differential braking and steer-by-wire together so that I can control steering angle and longitudinal velocity for better performance.

Differential braking systems typically utilize solenoid based on hydraulic modulator to change the brake pressures at the four wheels [22]. Torque balanced equations at four wheels, a four-degree-of-freedom tire model, are shown as

$$J_w \dot{\omega}_{fl} = T_{dfl} - T_{bfl} - R_{eff} F_{xfl}$$
$$J_w \dot{\omega}_{fr} = T_{dfr} - T_{bfr} - R_{eff} F_{xfr}$$
$$J_w \dot{\omega}_{rl} = T_{drl} - T_{brl} - R_{eff} F_{xrl}$$
$$J_w \dot{\omega}_{rr} = T_{drr} - T_{brr} - R_{eff} F_{xrr}$$

$$3.45$$

$T_{dfl}, T_{dfr}, T_{drl}, T_{drr}$ denote traction torque at each wheel, $T_{bfl}, T_{bfr}, T_{brl}, T_{brr}$ denote brake torque at each wheel. Braking force is defined to calculate brake torque, which is also the control variable applied at wheels,

$$T_{bfl} = F_{bfl} R_b$$
$$T_{bfr} = F_{bfr} R_b$$

$$3.46$$

$$T_{brl} = F_{brl}R_b$$

$$T_{brr} = F_{brr}R_b$$

R_b denotes brake radius, $F_{bfl}, F_{bfr}, F_{brl}, F_{brr}$ denote front left wheel brake force, front right wheel brake force, rear left wheel brake force and rear right wheel brake force.

3.5 State Space Model

Next step is to represent the state-space vehicle dynamics model for controller design. States from Eq. 3.29 and 3.30 contain longitudinal velocity, lateral velocity, yaw rate, roll angle, roll rate and angular velocity of four wheels. However, these parameters are not enough for some essential vehicle information such as locating a vehicle with position (X, Y) and yaw angle. They can be calculated through vehicle slip angle, longitudinal velocity, lateral velocity and yaw angle. Ideally the position at each sampling instant is calculated by the latter three variables without considering vehicle slip. However, the effect of slip could be significant for high-speed running vehicles because of the slip of tires. The vehicle slip angle is calculated as follows,

$$\beta = \tan^{-1}\frac{L_f \tan\delta}{L_f + L_r} \qquad\qquad 3.47$$

Therefore, the differential position expression is,

$$\dot{X} = v_x \cos(\beta + \psi)$$
$$\dot{Y} = v_x \sin(\beta + \psi)$$
$$\qquad\qquad 3.48$$

The integral of Eq. 3.48 is the X and Y value with respect to the inertial coordinate system.

Thus, the final expression of state vector is $x = [v_x, v_y, \dot{\psi}, \varphi, \dot{\varphi}, X, Y, \omega_{fl}, \omega_{fr}, \omega_{rl}, \omega_{rr}]$.

It is noted that the dynamic model developed is nonlinear. Some researchers tend to linearize nonlinear model for simplification [31,32], while the model here is hard to be linearized. Moreover, forced linearization can lead to too many assumptions prior to defining the model, so that the finalized model in such process would be inaccurate. In order to reduce the degree of nonlinearity, we can simplify the model appropriately. Assume that roll angle is small, so that $\sin \varphi \approx \varphi, \cos \varphi \approx 1$. Eq. 3.29 and 3.30 become,

$$
m \begin{bmatrix} \dot{v}_x - (v_y + 2\dot{\varphi}h)\dot{\psi} - h\varphi\ddot{\psi} \\ \dot{v}_y + v_x\dot{\psi} + h(\ddot{\varphi} - \dot{\varphi}^2\varphi - \varphi\dot{\psi}^2) \\ 0 \end{bmatrix}
$$
$$
= \begin{bmatrix} F_{xrl} + F_{xrr} + (F_{xfl} + F_{xfr})\cos\delta - (F_{yfl} + F_{yfr})\sin\delta \\ F_{yrl} + F_{yrr} + (F_{yfl} + F_{yfr})\cos\delta + (F_{xfl} + F_{xfr})\sin\delta \\ 0 \end{bmatrix}
$$

3.49

$$
M = \begin{bmatrix} \ddot{\varphi}I_{xx} - \dot{\psi}^2\varphi(I_{yy} - I_{zz}) \\ Neglected \\ \ddot{\psi}(\varphi^2 I_{yy} + I_{zz}) + 2\dot{\psi}\dot{\varphi}(I_{yy} - \varphi I_{zz}) \end{bmatrix} = \begin{bmatrix} M_x \\ M_y \\ M_z \end{bmatrix}
$$

3.50

Momentum equations are claimed clearly here for concluding before equations, Eq. 3.27 and 3.28 become,

$$
M_x = -\frac{F_{zl}L_w}{2} + \frac{F_{zr}L_w}{2} - mgH_{CG} + M_s
$$

3.51

$$
M_z = (F_{yrl} + F_{yrr})L_r - [(F_{yfl} + F_{yfr})\cos\delta + (F_{xfl} + F_{xfr})\sin\delta]L_f
$$

$$
+ (F_{xrl} + F_{xfl}\cos\delta - F_{yfl}\sin\delta)\left(\frac{L_w}{2} + h\varphi\right)
$$

3.52

$$
+ (F_{yrr}\sin\delta - F_{xfr}\cos\delta - F_{xrr})\left(\frac{L_w}{2} - h\varphi\right)
$$

Thus, the state space equation used for modeling the ego vehicle combines from Eq. 3.47 to 3.52,

$$\dot{x}_{k+1} = f(x_k, u_k) \tag{3.53}$$

$$\dot{v}_x = \left(v_y + 2\dot{\varphi}H_{CG}\right)\dot{\psi} + h\varphi\ddot{\psi} + \frac{F_x}{m} \tag{3.54}$$

$$\dot{v}_y = -v_x\dot{\psi} - H_{CG}\left(\ddot{\varphi} - \dot{\varphi}^2\varphi - \varphi\dot{\psi}^2\right) + \frac{F_y}{m} \tag{3.55}$$

$$\ddot{\psi} = \frac{M_z - 2\dot{\psi}\dot{\varphi}(I_{yy} - \varphi I_{zz})}{\left(\varphi^2 I_{yy} + I_{zz}\right)} \tag{3.56}$$

$$\ddot{\varphi} = \frac{M_x + \dot{\psi}^2\varphi(I_{yy} - I_{zz})}{I_{zz}} \tag{3.57}$$

$$\dot{X} = v_x \cos(\tan^{-1}\frac{L_f \tan\delta}{L_f + L_r} + \psi) \tag{3.58}$$

$$\dot{Y} = v_y \sin(\tan^{-1}\frac{L_f \tan\delta}{L_f + L_r} + \psi) \tag{3.59}$$

$$\dot{\psi} = \dot{\psi} \tag{3.60}$$

$$\dot{\varphi} = \dot{\varphi} \tag{3.61}$$

Equations below are extracted from tire model, which has four degrees of freedom,

$$\dot{\omega}_{fl} = (T_{dfl} - R_b F_{bfl} - RF_{xfl})/J_w$$

$$\dot{\omega}_{fr} = (T_{dfr} - R_b F_{bfr} - RF_{xfr})/J_w$$

$$\dot{\omega}_{rl} = (T_{drl} - R_b F_{brl} - RF_{xrl})/J_w \tag{3.62}$$

$$\dot{\omega}_{rr} = (T_{drr} - R_b F_{brr} - RF_{xrr})/J_w$$

In conclusion, the overall state equation is highly nonlinear and can be represented as follows,

$$\dot{x}(k) = f(x(k), u(k))$$

$$x(k+1) = f\big(x(k), u(k)\big)$$

<div align="right">3.63</div>

u denotes the inputs: steering angle and brake force at each wheel, that is, $u = [\delta, F_{bfl}, F_{bfr}, F_{brl}, F_{brr}]$. Index k denotes current sampling instant since the controller designed in next chapter is discrete.

The output vector is $y = [X, Y, \psi]^T$, while ψ is related to steering angle and slip angle,

$$\psi = \delta - \frac{\alpha_f + \alpha_r}{2}$$

<div align="right">3.64</div>

CHAPTER 4 MOTION CONTROL

Considering the rollover prevention problem, which is actually a decision-making process for vehicle equipped with ADAS features. Currently, ADAS system of most commercial vehicles on the market have limitations. For example, most ADAS features only take one parameter into consideration, such that Adaptive Cruise Control (ACC) system only controls vehicle velocity; Lane Keeping System (LKS) only controls the steering angle to keep the ego vehicle on the center of lane. However, with the increasing of demands as well as the improvement of sensors such as radars, LiDARs, cameras, GPS/INS units and odometry, one parameter controlled is not enough to further develop vehicle industry. Meanwhile, the increasing accuracy and computational power of ADAS processors can handle more complicated use cases.

For the rollover prevention problem, the overall decision-making architecture of any ADAS features is defined in [22], which can be decomposed into four components: Route Planning, Behavioral Layer Decision Making, Motion Planning and Local Feedback Control. Route Planning is to find a minimum-cost path on a known map, which can be either from a combination of perception from sensors, as well as localization information from GPS or SLAM. Behavioral Layer is to decide patterns cruise-in-lane, change-lane, or turn-right, the ego vehicle should choose from perceived agents' obstacles and signage. Motion Planning is to plan a path or trajectory considering soft and hard constraints in the environment. The planned path or trajectory will be executed by a feedback controller to carry out the motion and tracking errors. The final two steps can be summarized into one step called Motion Control.

Basically, Motion Control includes two sections: one is path planning, the other one is path tracking or following. Model Predictive Control (MPC) has been popular in industry for a long time [26]. The key feature of MPC is explicit use of a dynamical process model for controlled variable prediction at a future time horizon and calculation of a control actions to minimize a cost function [24]. It can be used for both application, path planning as a planner and path tracking as a controller. It optimizes a performance cost satisfying the physical constraints, which is initialized by the real measurements, to obtain a sequence of control moves or control laws [25]. Dynamics model developed in Chapter 3 is nonlinear, presenting nonlinear state-space equation, which requires a nonlinear model predictive control controller for path tracking. Current nonlinear MPC can handle high nonlinearity well, so there is no need to further linearize the nonlinear problem, which might have negative effect on the accuracy of the problem. Nonlinear model predictive control, or NMPC, is a variant of model predictive control (MPC) that is characterized by the nonlinear system models in the prediction [26]. NMPC executes the iterative solution of optimal control problems on a specific prediction horizon. Several optimal control methods are used to get the numerical solution of the NMPC, including single shooting and multiple shooting methods. These optimal control methods indicate the optimal control problem is transformed to nonlinear programming program.

4.1   Optimization

Model Predictive Control is strongly related to the optimal control since the control algorithms are based on solving an optimization problem numerically at each step for a discrete-time or continuous-time system. Optimization problem of MPC can be divided

into two categories, unconstrained and constrained. Typically, a Quadratic Programming or Linear Programming problem, respectively. Classical methods utilized to solve discrete-time optimization are 1) Symbolic Differentiation and 2) Numerical Differentiation. However, both methods have difficulty in calculating higher derivatives, meaning that they can be slow when computing the derivatives of a function with multiple inputs. Especially, it is difficult for human programmers to get an explicit Jacobian Matrix for the state-space equation represented in Chapter 3. Thus, a more effective method called Automatic Differentiation (AD) is introduced as a technique to evaluate the derivative of a function, regardless of how complicated the algorithm is. Decomposition using chain rule is the fundamental of AD. For example,

$$y = f(x) = f(w_1) = w_2 \tag{4.1}$$

then from chain rule we can get

$$\frac{dy}{dx} = \frac{dy}{dw_1}\frac{dw_1}{dx} \tag{4.2}$$

Usually, there are two modes of AD: forward accumulation and reverse accumulation. The differences between these two modes is the calculation order: forward accumulation traverses it from inside to outside, while reverse accumulation does the contrary. Forward accumulation is easier to be implemented as the flow of derivative information along with the order compared with reverse accumulation, in which case, the derivative of multiple variables as a Jacobian matrix can be calculated by AD. Jacobian matrix is used to represent the relationship between the current state and current state derivative. Unlike linear models, the input and output cannot be expressed as follows,

$$y = Ax + Bu \qquad\qquad\qquad 4.3$$

In Eq. 4.3, A and B are numerical matrix.

Currently, many open-source AD software tools have been developed, including ACADO Toolkit, DIRCOL, DyOS and MUSCOD-II [28], wherein, CasADi, provides efficient solutions of nonlinear optimization problems as well as dynamic optimization problem. The CasADi project was started by Joel Andersson and Joris Gillis of the KU Leuven under supervision of Moritz Diehl [28]. Compared with other tools, CasADi allows users to implement their own methods with multiple decision variables and multi-dimensional vectors, rather than giving an unknown Optimal Control Problem (OCP) solver. Also, CasADi has several software interfaces and programming languages applied, such as C++, Python and MATLAB/SIMULINK. The core of CasADi is the unique self-defined framework that users can build their own OCP by constructing symbolic expressions. More details of CasADi and its implementation will be discussed in Chapter 5 Simulation.

4.2 Solution for Nonlinear Model Predictive Control

The MPC/NMPC mathematical formulation contains four relative parts,

Table 3. MPC Mathematical Formulation

Running (stage) Costs	Characterize the control objective
Cost Function	Evaluation of the running costs along the whole prediction horizon

Optimal Control Problem	To find a control sequence with respect to the minimizing cost
Value Function	Minimum of the cost function

Table 3 shows that Running Costs is an equation of time because the prediction horizon is time based. At each sample time, Cost Function is a sequence or sum of Running Costs equations, which is to determine a sequence of *control moves*, in other words, manipulated input changes. Optimal Control Problem is to minimize the cost function, and value function is the minimum of the cost function. In general, the MPC calculations are based on current measurements and predictions of the future values of the outputs [29] regarding to optimal control problem with subjecting to state space equation and physical constraints and soft constraints. The physical constraints are usually defined as input constraints and soft constraints are defined as state constraints and output constraints. Physical constraints should be strictly obeyed while soft constraints can be violated if they are inconsistent with physical constraints. The overall picture of MPC is shown in Figure 10. Basic concept for model predictive control.
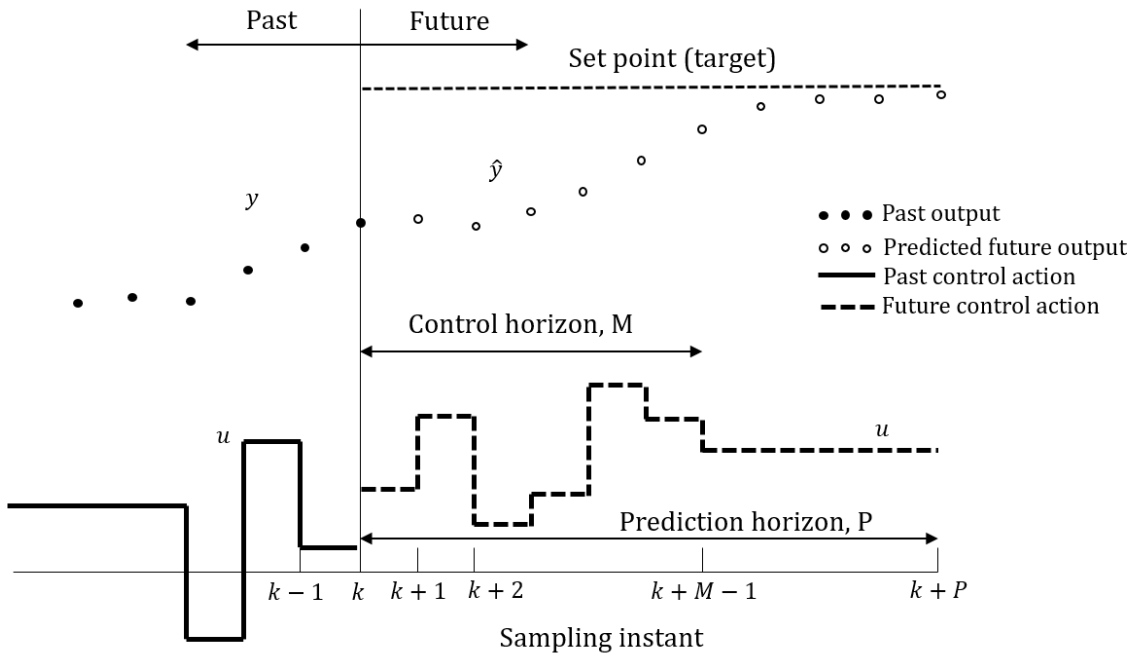
Figure 10. Basic concept for model predictive control

In Figure 10, the target (final) point is given by GPS mapping and for actual situations as reference, k denotes the current sampling instant, so input $u(k)$ and output $y(k)$ are measurements and known. Through the *control horizon M*, the MPC calculates the input $\{u(k + i - 1), i = 1,2,3, \dots, M\}$ at each sample time until *M*, as well as the output $\{\hat{y}(k + i), i = 1,2,3, \dots, P\}$ at each sample time through the *prediction horizon P* regarding to the optimal control problem. The input is held constant as the previous move value until next move. As mentioned above, the key feature of MPC is the *receding horizon*, only the first move $(x(k), y(k))$ is the current measurement and implemented, then a new sequence of input and output changes is calculated at next sample time when the object has arrived at the next point, which means the next move is the new measurement and it will be used as the first move in the next computation. This procedure is repeated at each sample time.

For this research, the output is the state parameters of the object vehicle. However, since the most important parameters of the vehicle are the position and yaw angle of vehicle or named posture of vehicle (X, Y, ψ). The posture is applied to cost function and recorded as changing variables. The input is a vector containing steering angle and brake pressures acted at four wheels. The corresponding equations for the four concepts in Table 3 are shown in Table 4,

Table 4. Specific Problem using MPC Mathematical Formulation

Running (stage) Costs	$\left\|y(k) - y_{ref}(k)\right\|_Q^2 + \|\Delta u(k)\|_R^2$
Cost Function	$$\sum_{i=1}^{N_P}\left\|y(k+i\|k) - y_{ref}(k+i\|k)\right\|_Q^2$$ $$+ \sum_{i=1}^{N_c-1} \|\Delta u(kk+i\|k)\|_R^2$$
Optimal Control Problem	$$\min_{X(.),Y(.),\psi(.),u(.)}\left(\sum_{i=1}^{N_P}\left\|y(k+i\|k) - y_{ref}(k+i\|k)\right\|_Q^2\right.$$ $$\left. + \sum_{i=1}^{N_c-1} \|\Delta u(k+i\|k)\|_R^2\right)$$
Value Function	$$J(x(.),u(.)) = \min_{X(.),Y(.),\psi(.),u(.)}\left(\sum_{i=1}^{N_P}\|y(k+i\|k)\right.$$ $$\left. - y_{ref}(k+i\|k)\right\|_Q^2 + \sum_{i=1}^{N_c-1} \|\Delta u(k+i\|k)\|_R^2\right)$$

N_p denotes the prediction horizon, N_c denotes the control horizon. Q and R denote the

weighting matrices of states and control actions, respectively. These two weighting matrices can be tuned because the weight of each variables is roughly chosen as initial values and finally decided based on the simulation results. Index k denotes the current sampling instant; i denotes the next predicted sample time; Δu denotes the difference between the control variables at current sample time and that at next sample time; x_{ref} denotes the state reference. As mentioned above, an optimal control problem usually subjects to physical constraints for inputs constraints and soft constraints for state or output constraints.

Thus, the MPC problem with respect to constraints can be represented in the following form,

$$\min_{X(.),Y(.),\psi(.),u(.)} (\sum_{i=1}^{N_P} \left\| y(k+i|k) - y_{ref}(k+i|k) \right\|_Q^2$$

s.t.
$$+ \sum_{i=1}^{N_c-1} \left\| \Delta u(k+i|k) \right\|_R^2)$$

$$\dot{x}(k) = f(x(k), u(k))$$

$$u_{min} \le u \le u_{max}$$

$$x_{min} \le x(k) \le x_{max}$$

$$y_{min} \le y \le y_{max}$$

4.4

This thesis focuses on Case 1 in Chapter 2. The specific problem in Case 1 is how to avoid collision as well as rollover. Therefore, the cost function is to minimize the error of position and heading angle (also yaw angle) with respect to the reference, plus the minimization of change in the steering angle from one-time step to the next. Because if the

steering wheel is turned sharply, the ride may become uncomfortable for the passengers and the possibility of rollover may increase as well. The control action vector is $u = [\delta, F_{fl}, F_{fr}, F_{rl}, F_{rr}]^T$, state vector is $x = [v_x, v_y, \dot{\psi}, \varphi, \dot{\varphi}, X, Y, \omega_{fl}, \omega_{fr}, \omega_{rl}, \omega_{rr}]^T$. Input constraints consist of maximum steering angle, minimum steering angle, maximum brake forces and minimum brake forces. Differential equation determines the MPC problem to be nonlinear because state space equation is nonlinear but need to be followed. State constraints consist of maximum longitudinal velocity, minimum velocity, maximum yaw rate, minimum yaw rate, maximum roll angle, minimum roll angle, maximum roll rate and minimum roll rate. Output constraints consist of minimum and maximum changes of longitudinal position, lateral position and yaw angle within one sampling instant, respectively.

$$\min_{X(.),Y(.),\psi(.),u(.)} \left(\sum_{i=1}^{N_P} \left\| y(k+i|k) - y_{ref}(k+i|k) \right\|_Q^2 \right.$$

s.t.

$$\left. + \sum_{i=1}^{N_c-1} \left\| \Delta u(k+i|k) \right\|_R^2 \right)$$

$$\dot{x}(k) = f(x(k), u(k))$$

$$0 < v_x \le v_{max}$$

$$\dot{\psi}_{min} \le \dot{\psi} \le \dot{\psi}_{max}$$

$$\varphi_{min} \le \varphi \le \varphi_{max}$$

$$F_{bmin} \le F_b \le F_{bmax}$$

$$\delta_{min} \le \delta \le \delta_{max}$$

4.5

$$\Delta X_{min} \leq \Delta X \leq \Delta X_{max}$$

$$\Delta X_{min} \leq \Delta Y \leq \Delta X_{max}$$

$$\Delta\psi_{min} \leq \Delta\psi \leq \Delta\psi_{max}$$

$$-1 < LTR < 1$$

In Eq. 4.5, LTR stands for Load Transfer Ratio, which is an index to determine whether the vehicle will rollover or not. Usually, one side wheels lift-off will be considered as the index for high rollover possibility in industry. In other words, the vertical forces in one side will be zero once lift-off happens. It is calculated by using vertical forces acted at wheels using Eq. 3.26,

$$LTR = \frac{F_{zfr} + F_{zrr} - F_{zfl} - F_{zrl}}{F_{zfl} + F_{zrl} + F_{zfr} + F_{zrr}} \qquad 4.6$$

The value of LTR would be -1 or 1 when lift-off takes place. Eq. 4.6 can be further simplified as below,

$$LTR = \frac{2H_{CG}a_y}{L_w g} \qquad 4.7$$

But note that the way in Eq. 3.26 does not consider the roll influence, thus, to take roll motion into consideration, a balanced torque equation of the unsprung mass over the roll axis is represented as,

$$-\frac{F_{zl}L_w}{2} + \frac{F_{zr}L_w}{2} + K\varphi + c\dot\varphi = 0 \qquad (4.8)$$

$$LTR = \frac{2}{mgL_w}(K\varphi + c\dot\varphi) \qquad (4.9)$$

There are two approaches to demonstrate the capability of controller in tracking and respecting constraints, one is setting the initial point and goal point, then the NMPC controller will estimate intermediate states between the initial position and goal position. A trajectory is planned with respect to various constraints defined above; the other is to design a trajectory that is complicated and NMPC controller controls the vehicle follow the path. The test and verify will be demonstrated in next chapter.

CHAPTER 5 RESULTS & SIMULATION

The simulation of vehicle rollover prevention problem will be conducted based on the vehicle dynamics model discussed in previous chapters. Before constructing a nonlinear programming problem, we should be aware of vehicle dynamics parameters [33].

Table 5. Vehicle Parameters

Parameters	Conception	Value	Unit
L_f	Length from center of gravity to front axle	1.34	m
L_r	Length from center of gravity to rear axle	1.50	m
L_w	Wheelbase	2.00	m
m	Vehicle mass	2500	kg
g	Gravity acceleration	9.8	kg/m^2
H_{CG}	Height of center of gravity	1.0	m
I_{xx}	Moment of inertia about x axle	3911	kg.m^2
I_{yy}	Moment of inertia about y axle	3911	kg.m^2
I_{zz}	Moment of inertia about z axle	751	kg.m^2
K	Spring constant of suspension system	79000	N/m
c	Damping constant of suspension system	8038	Ns/m
R_b	Brake radius	0.28	m
C_α	Longitudinal stiffness of tire	62192	N/rad
C_λ	Lateral stiffness of tire	60000	N/rad
J_w	Tire moment of inertia	0.34	kg m^2

The values in Table 5 are estimated according to actual light trucks. Constraints in Eq. 4.5 are defined in Table 6 according to the specific situation (avoid collision as well as rollover) and empirical values,

Table 6. Hard and soft constraints values of optimization problem

Parameters	Conception	Value	Unit
v_{max}	Maximum longitudinal velocity	26	m/s
$\dot{\psi}_{max}$	Maximum yaw rate	$\dfrac{\pi}{4}$	rad/s
φ_{min}	Minimum roll angle	$-\dfrac{\pi}{6}$	rad
φ_{max}	Maximum roll angle	$\dfrac{\pi}{6}$	rad
F_{bmax}	Maximum brake force	600	N
F_{bmin}	Minimum brake force	-600	N
δ_{min}	Minimum steering angle	$-\dfrac{\pi}{4}$	rad
δ_{max}	Maximum steering angle	$\dfrac{\pi}{4}$	rad
ΔX_{min}	Minimum change of longitudinal position at one sample time	0	m
ΔX_{max}	Maximum change of longitudinal position at one sample time	1	m
ΔY_{min}	Minimum change of lateral position at one sample time	-1	m
ΔY_{max}	Maximum change of lateral position at one sample time	1	m
$\Delta\psi_{min}$	Minimum change of yaw angle at one sample time	$-\dfrac{\pi}{6}$	rad
$\Delta\psi_{max}$	Maximum change of yaw angle at one sample time	$\dfrac{\pi}{6}$	rad

Minimum braking force is negative because the algorithm takes acceleration into consideration to keep the longitudinal velocity of vehicle larger than 10 m/s. During this process, a differential splits power between the left and right halves of a car's driven axle(s) and allows either half of the axle to rotated at a different speed than the other. Low speed simultaneously brings issues of traffic jam or other collision issues. Thus, it could be necessary for maintaining traction in changing lane.

The remaining variables of controller are defined here:

Sample time $T = 0.2$, prediction horizon $N_p = 10$, control horizon $N_c = 10$, weighting matrix $Q = [0\ 1.0^{-1}; 0\ 1.0^{-3}]$, $R = [1.0^{-1}\ 0\ 0\ 0\ 0; 0\ 1.0^{-3}\ 0\ 0\ 0; 0\ 0\ 1.0^{-3}\ 0\ 0; 0\ 0\ 0\ 1.0^{-3}\ 0; 0\ 0\ 0\ 0\ 1.0^{-3}]$.

One of the goals of this simulation is to minimize position and yaw angle errors with respect to the reference value. The overall simulation environment in CasADi [27] is,
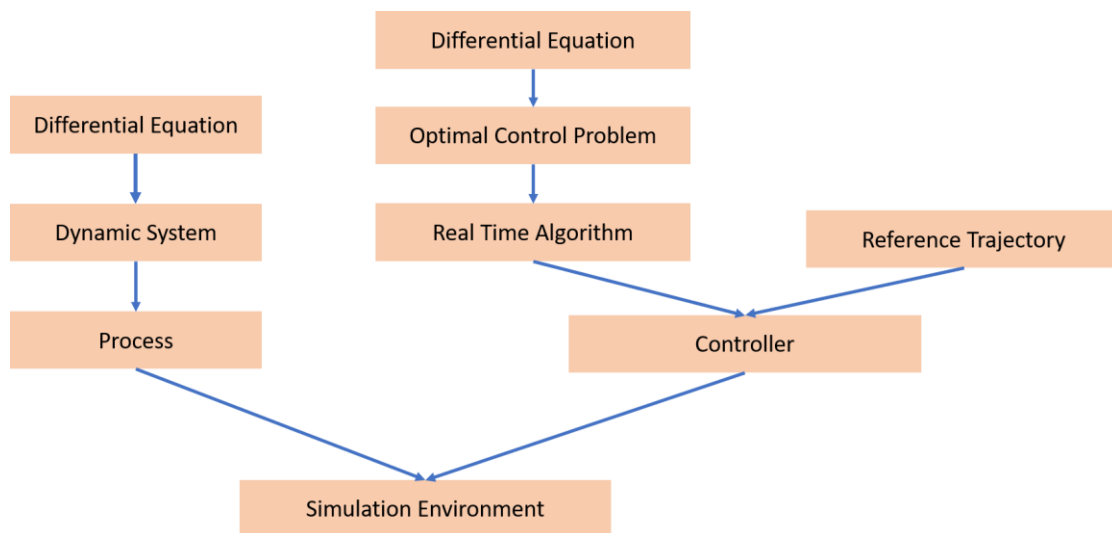
Figure 11. Simulation Environment

Differential equation, optimal control problem, dynamic system and real-time algorithm

for optimization have been declared in previous chapters. Reference trajectory is currently needed before path tracking. There are two methods to test and verify the trajectory tracking capability by setting two different types of reference value: providing initial posture and goal posture or providing entire path from initial point to final point. The former one is preferred in this thesis, since it can achieve motion planning by generating path and trajectory (containing speed profile) and tracking trajectory.

There are several scenarios that can be built, but basically seven scenarios simulated for benchmark: 1) no obstacle, 2) the obstacle position is set as [10;0.0], goal position is set as [20;2.0], 3) the obstacle position is set as [10;0.0], goal position is set as [20;2.5], 4) the obstacle position is set as [10;0.0], goal position is set as [30;2.0], 5) the obstacle position is set as [10;0.0], goal position is set as [30;2.5], 6) same condition as 2) but the vehicle has higher center of gravity 1.2m, 7) same condition as 4) but the vehicle has higher center of gravity 1.2m. Scenario 1 shows that the algorithm is constructed correctly at the initial state. Scenarios 2 to 5 are used to research the stability of controller. Scenarios 6 and 7 are used to find the effect of high center of gravity. I have tried to build a scenario that goal position is set as [20;3], but the controller failed planning a path for the vehicle to follow, which means rollover is impossible to avoid in some specific scenarios. This would be the future work on trade-off between rollover and collision prevention. Figure 12 shows the vehicle rollover without any controller at 26 m/s speed. Upper image in Figure 12 is plotted using PreScan by given a trajectory. The results in scenario 1 show that the algorithm can give a best and reasonable solution without deceleration if there is no obstacle. The results in scenarios 2-5 show that the controller is relatively stable within acceptable tolerance by

moving the y position forward. The results in scenarios 2 and 6, 4 and 7 show that the controller is able to handle the high center of gravity.
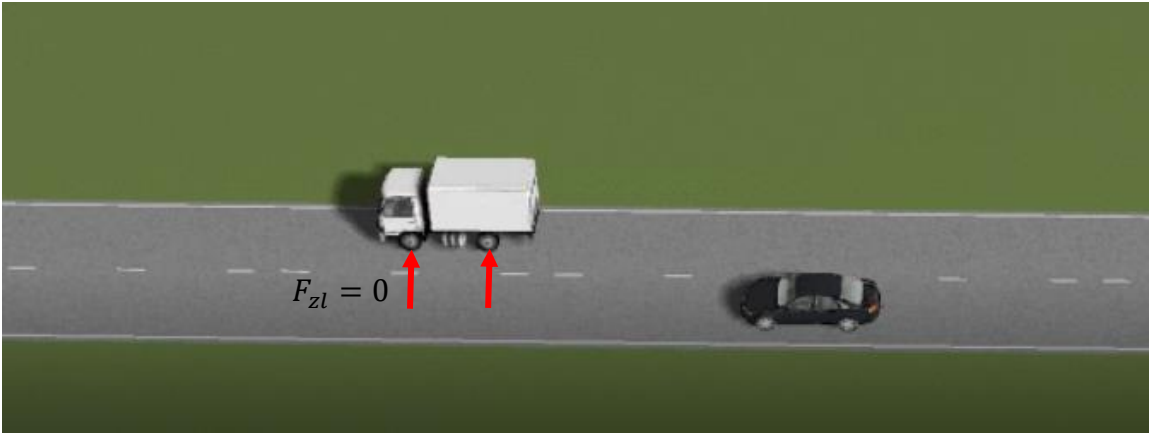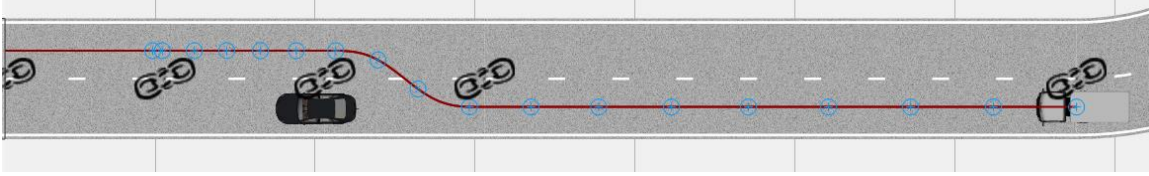
Figure 12. Rollover situation
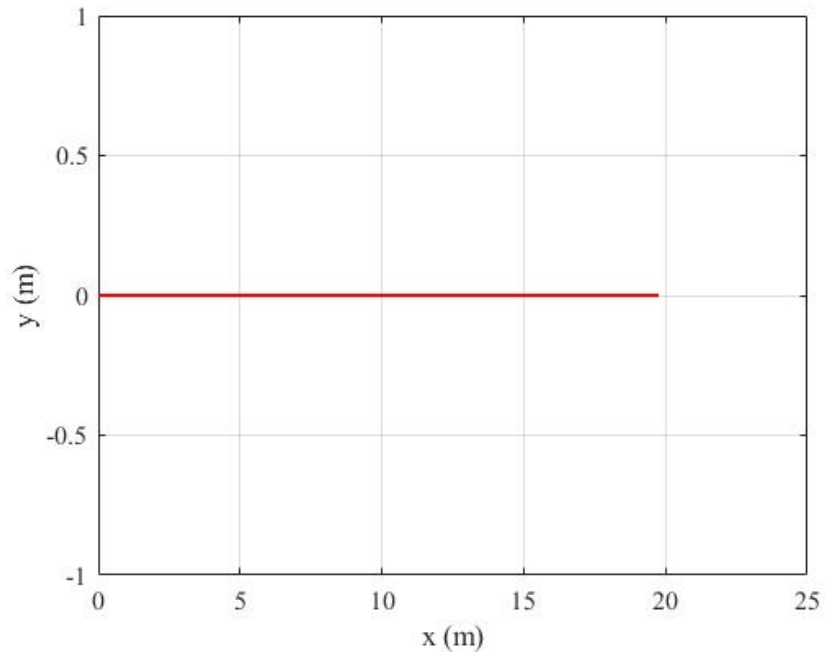
1. **No obstacle**

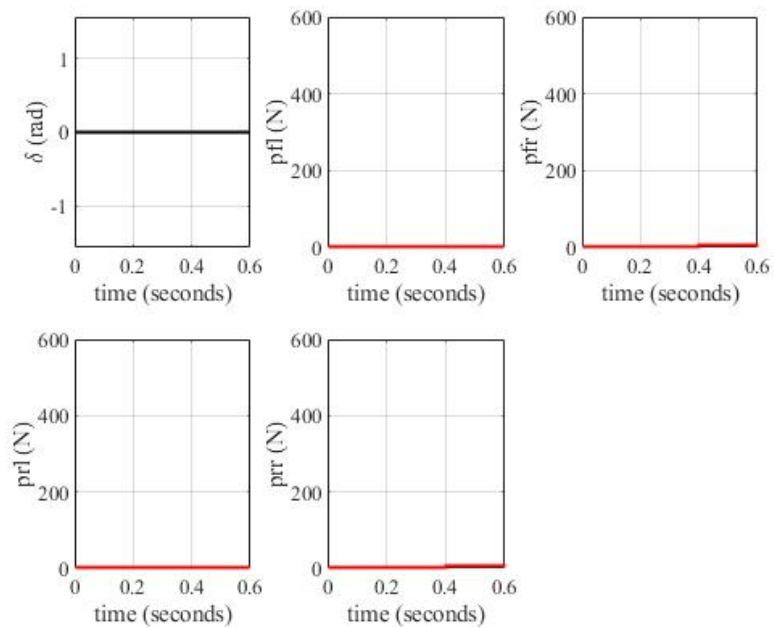Figure 13. Scenario 1: No obstacle – posture of vehicle
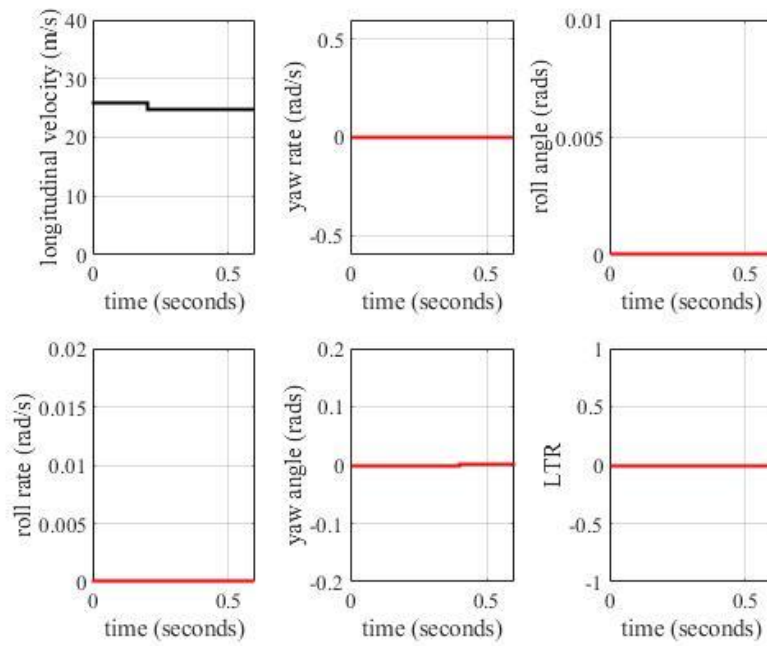

Figure 14. Scenario 1: No obstacle - control actions

Figure 15. Scenario 1: No obstacle – vehicle states

2. Obstacle position is [10;0], goal position is [20;2.0]

In Figure 16, the green box stands for the obstacle, which has same meaning in following

figures.
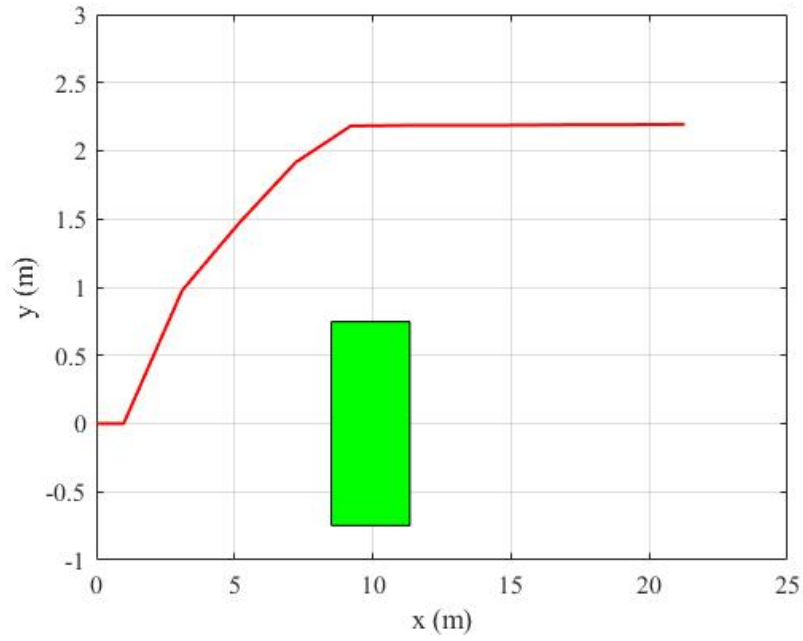
Figure 16. Scenario 2: Posture of vehicle
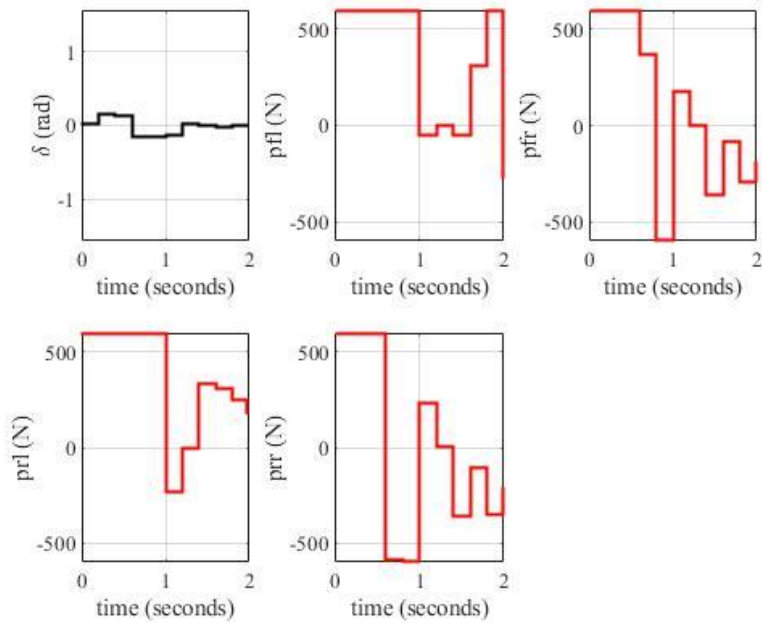
Figure 17. Scenario 2: Control variables
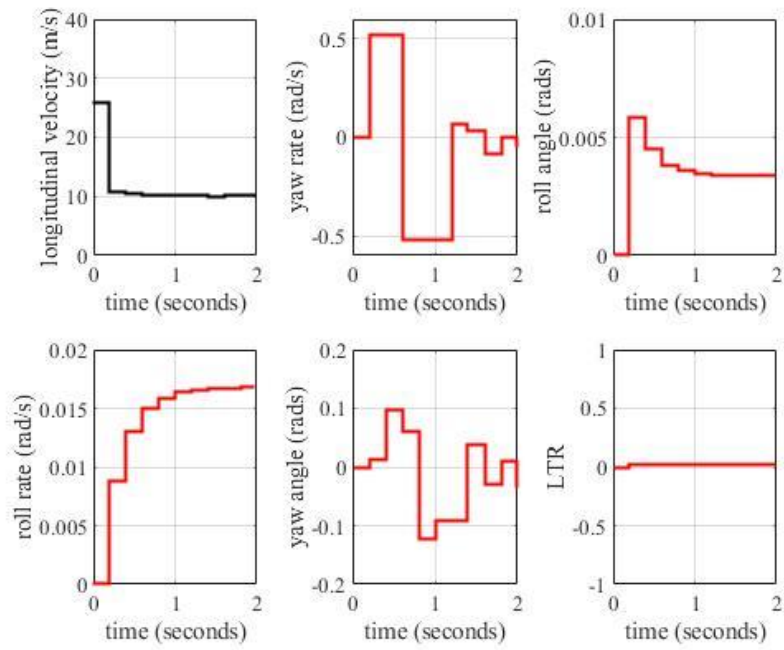
Figure 18. Scenario 2: Vehicle states

3. Obstacle position is [10;0], goal position is [20;2.5]
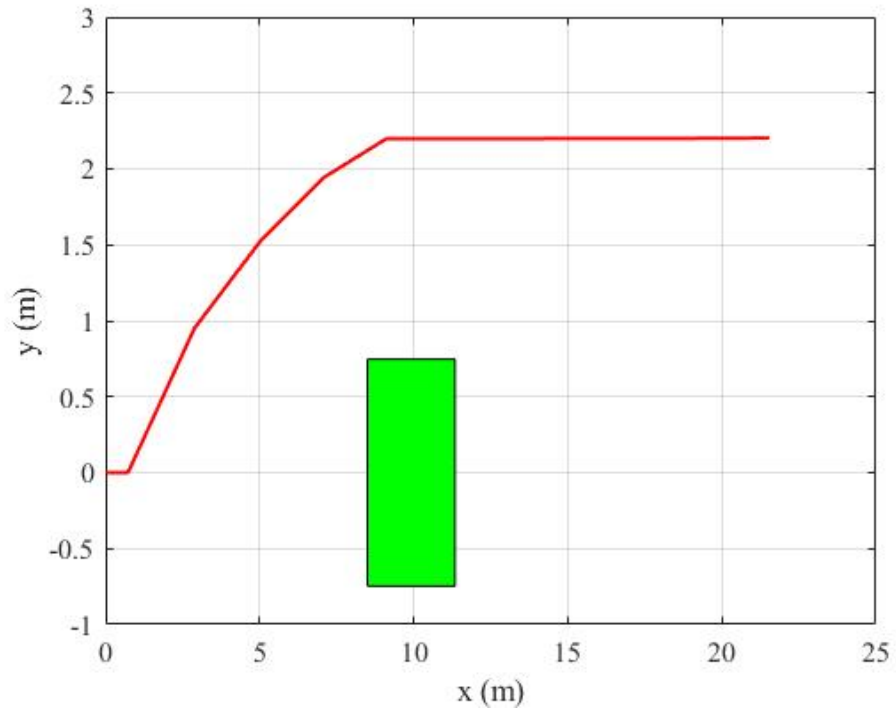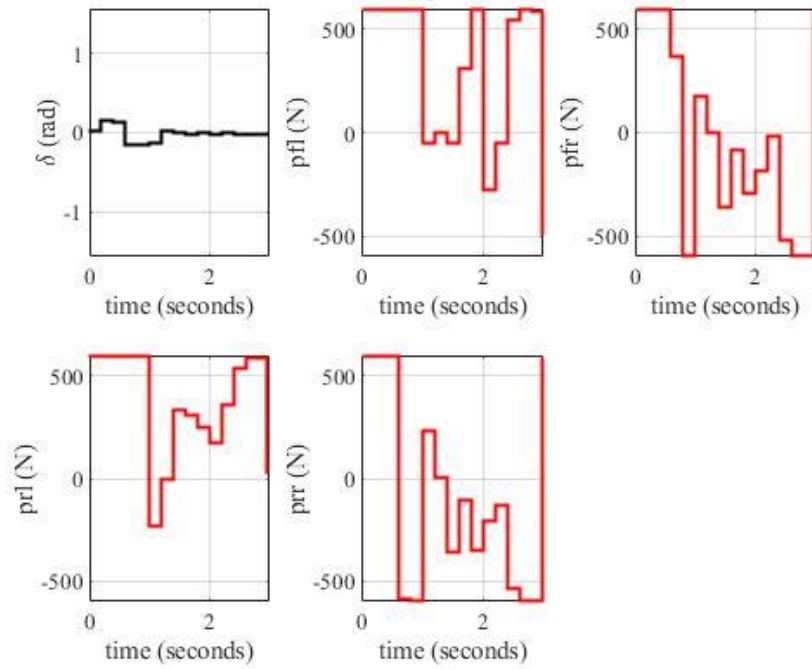
Figure 19. Scenario 3: Posture of vehicle

From scenario 2 and scenario 3, we can know that within certain velocity.
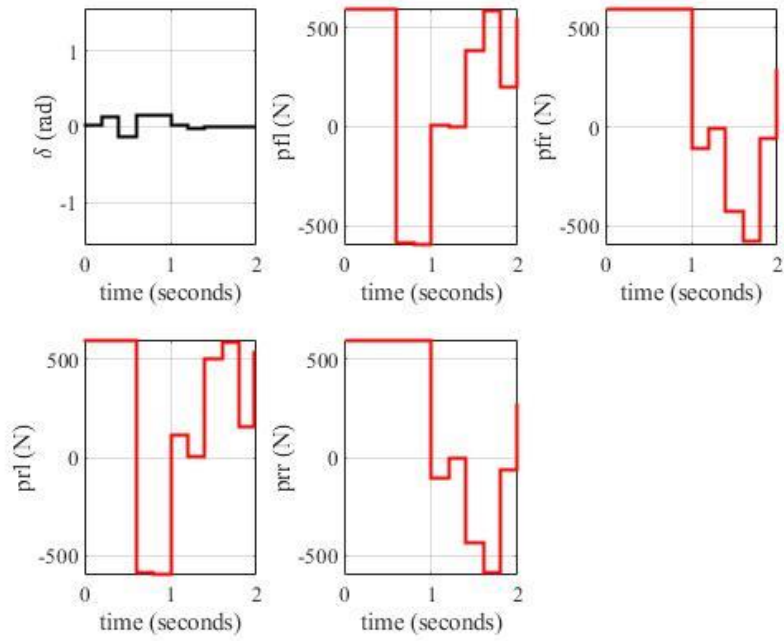
Figure 20. Scenario 3: Control variables
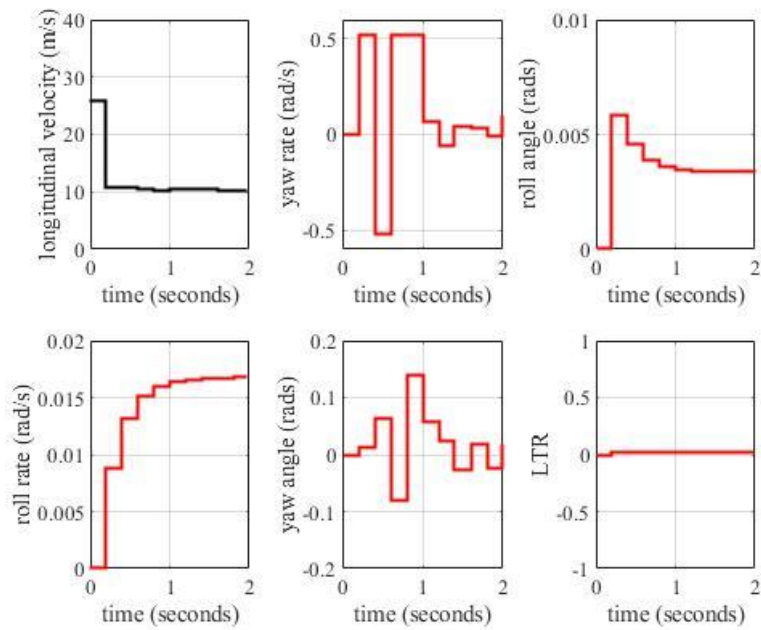
Figure 21. Scenario 3: Vehicle states

4. Obstacle position is [10;0], goal position is [30;2]
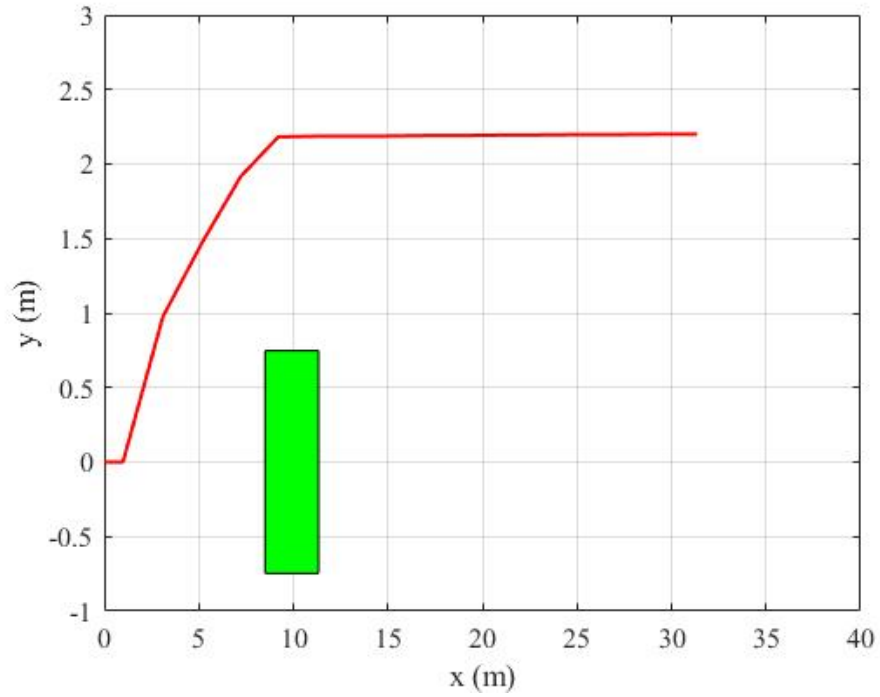
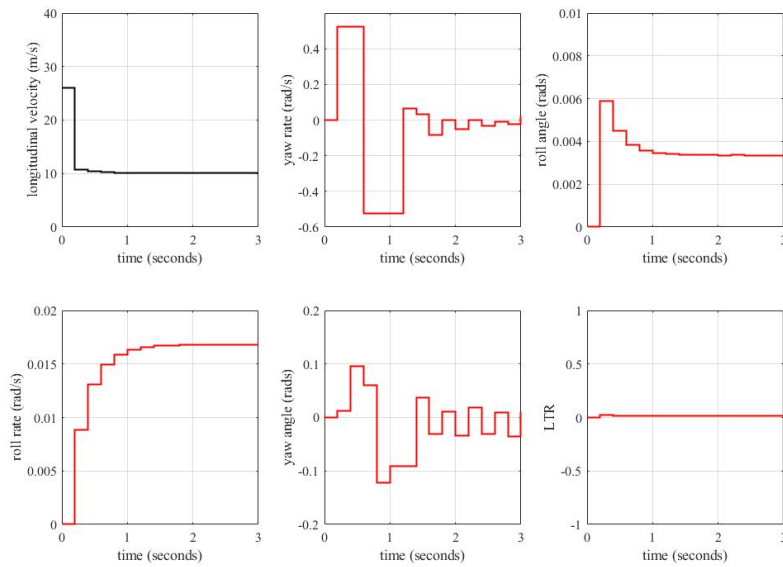Figure 22. Scenario 4: Posture of vehicle

Figure 23. Scenario 4: Control variables

Figure 24. Scenario 4: Vehicle states

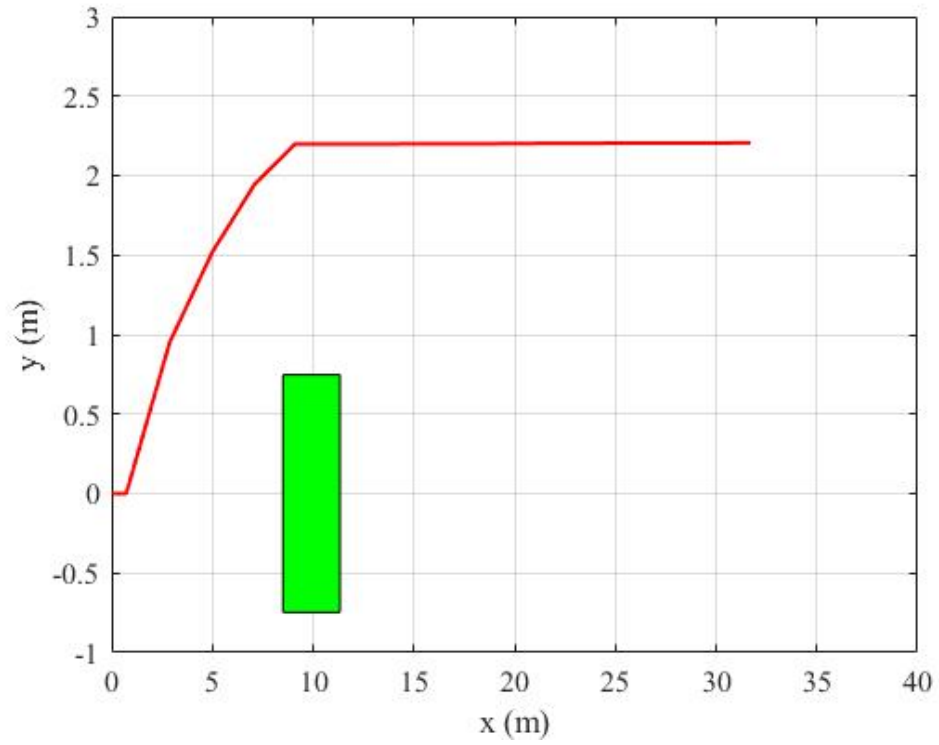**5. Obstacle position is [10;0], goal position is [30;2.5]**
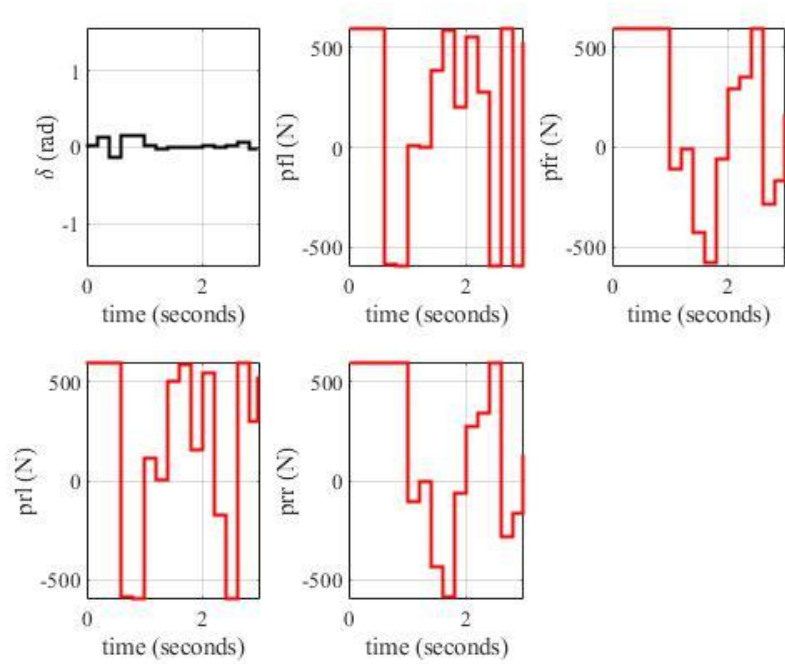

Figure 25. Scenario 5: Posture of vehicle
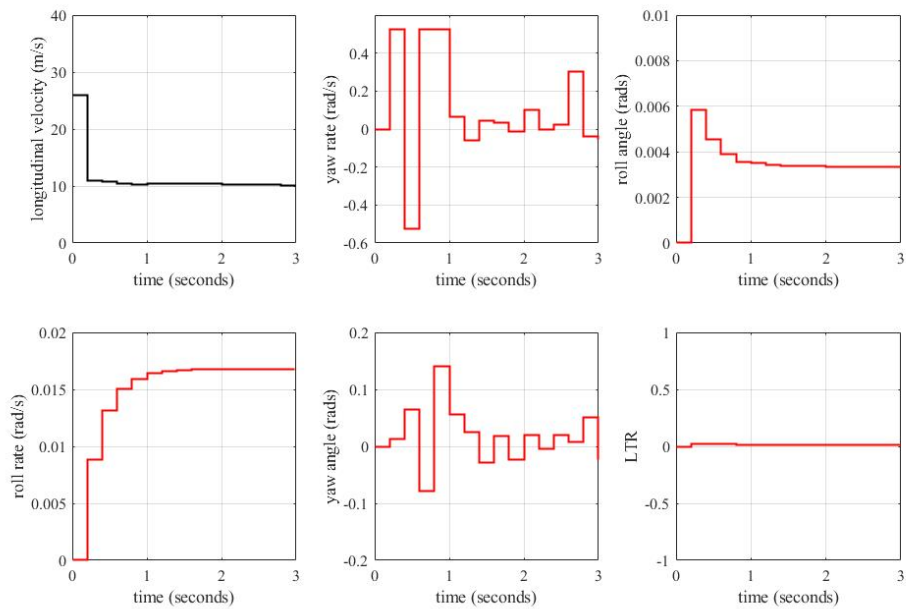
Figure 26. Scenario 5: Control variables

Figure 27. Scenario 6: Vehicle states

6. Obstacle position is [10;0], goal position is [20;2.0] with higher center of gravity of 1.2m
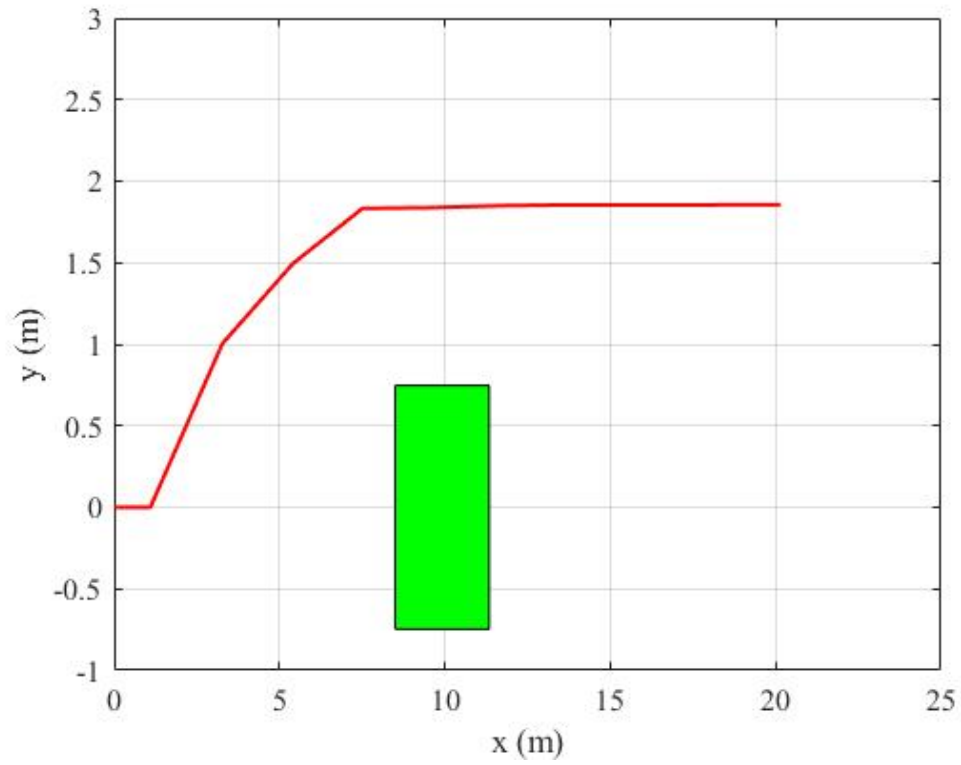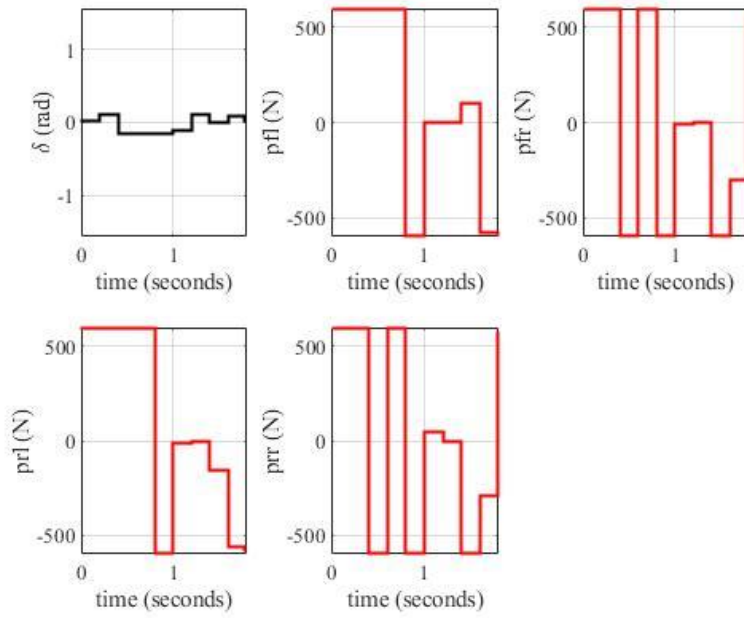

Figure 28. Scenario 6: Posture of vehicle

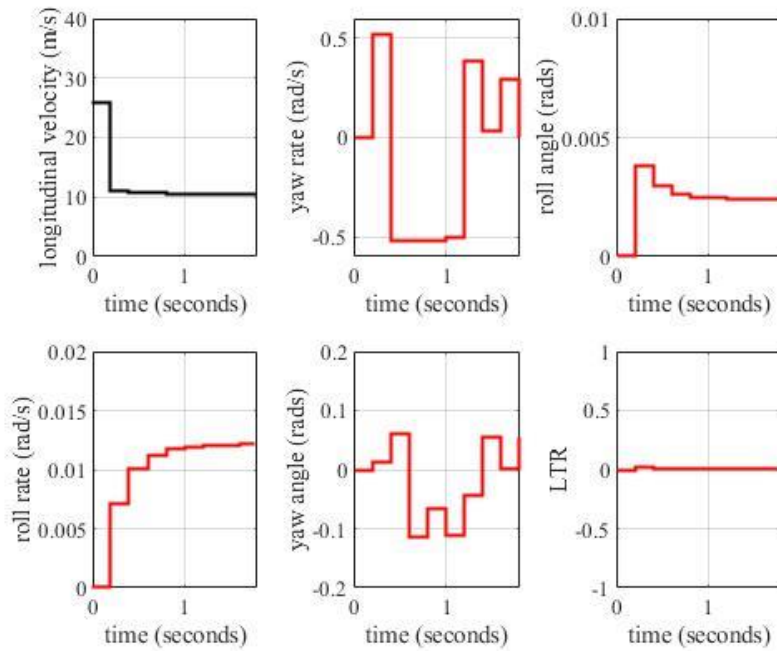Figure 29. Scenario 6: Control variables

Figure 30. Scenario 7: Vehicle states

7. Obstacle position is [10;0], goal position is [30;2.0] with higher center of gravity of 1.2m
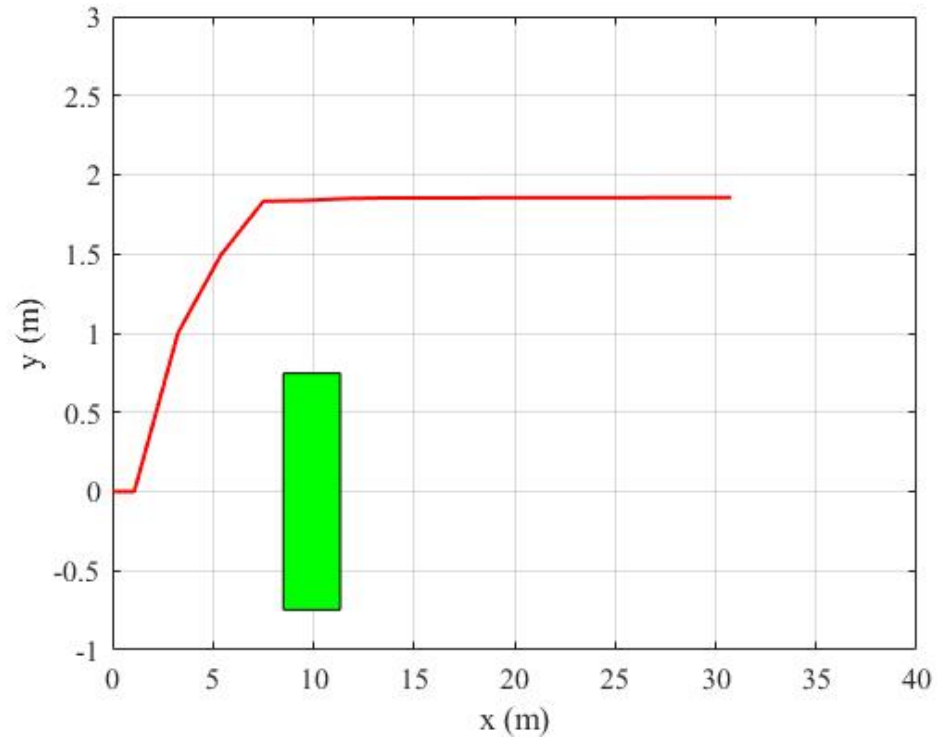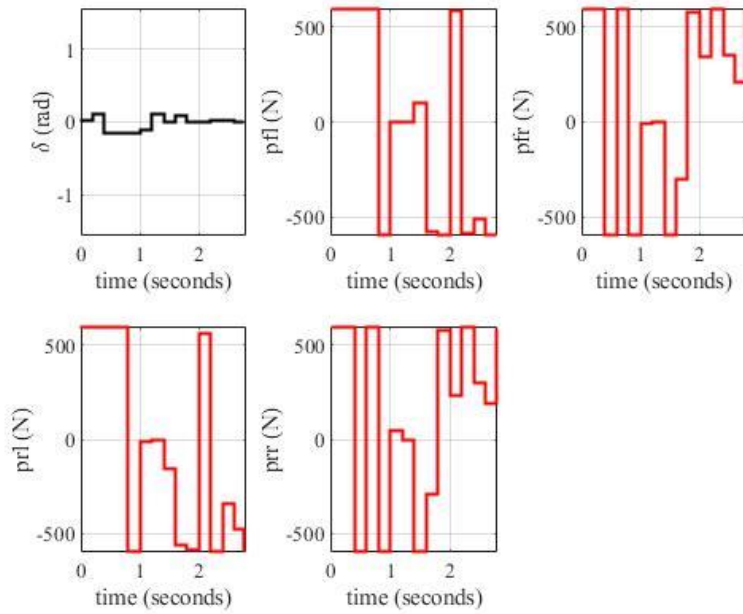

Figure 31. Scenario 7: Posture of vehicle
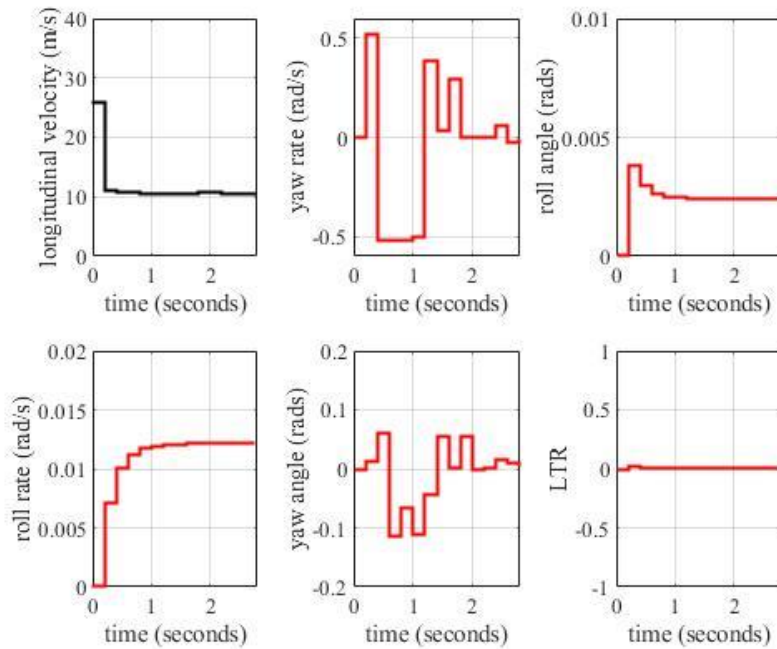
Figure 32. Scenario 7: Control variables

Figure 33. Scenario 7: Vehicle states

CHAPTER 6 CONCLUSION AND FUTURE WORK

This thesis presents a rollover prevention method using model predictive control while taking sensor information into consideration. It is a challenge to combine complicated vehicle dynamics model and path planning and tracking together, in which case the controller needs to comply with various soft and hard constraints. The vehicle model used in this thesis contains both lateral dynamics and longitudinal dynamics, plus degree of freedom of roll motion. Moreover, nonlinear model brings more challenges on problem formulation and programming and more requirements on computing power. Since all the cases in consideration are in fast maneuver, a robust system is a must, or the varying environment will lead to wrong and dangerous decisions.

To conclude, this thesis analyzes different scenarios where vehicles may involve making a decision. Then, a four-degree-of-freedom nonlinear vehicle dynamics model is developed, which provides state-space equations for the controller design. A nonlinear model predictive control is chosen in this thesis because its advantages in multiple inputs and multiple outputs system and nonlinear programming problem solving capability with respect to soft constraints. CasADi is used for simulation of path tracking because of its strong ability in solving optimal control problem (OCP) by multiple shooting technique to nonlinear programming problem (NLP) The results in Chapter 5 test and verify the powerful potential of the proposed method for tracking path in intensive computation when solving NLP.

Path planning and path following can be implemented using one controller in this thesis. The controller is evaluated off-line and ensure robustness of the controller to some extent.

In the future work, instead of only considering the preceding vehicle and existing constraints, all-surrounding vehicle information can be captured in order to assist vehicles make an optimal decision for collision and rollover prevention at real time, which requires more robust algorithm and powerful hardware.

REFERENCES

[1] American Automobile Association. (2019). 2019 ADAS technology research report. Retrieved from

https://www.aaa.com/AAA/common/AAR/files/ADAS-Technology-Names-Research-Report.pdf.

[2] National Highway Traffic Safety Administration (2013). Traffic Safety Facts.

[3] Shim, T. and Toomey, E. D. (2004). Investigation of Active Steering/Wheel Torque Control at the Rollover Limit Maneuver. *SAE 2004 Automotive Dynamics, Stability & Controls Conference and Exhibition*, May 2004.

[4] Wang, F. and Chen, Y. (2017). Vehicle Rollover Prevention Through A Novel Active Rollover Preventer. *ASME 2017 Dynamic Systems and Control Conference*, October 2017.

[5] U.S. Department of Transportation. (n.d.). Retrieved from

https://www.safercar.gov/Vehicle-Shoppers/Rollover/Causes

[6] Heydari, M., Dang, F., Goila, A., Wang, Y. and Yang, H. (2017). A Lane Departure Estimating Algorithm Based on Camera Vision, Inertial Navigation Sensor and GPS Data. *SAE Technical Paper*, March 2017.

[7] Pepy, R., Lambert, A. and Mounier, H. (2006). Path Planning using a dynamic vehicle model. *2006 2nd International Conference on Information & Communication Technologies*, April 2006.

[8] Honc, D., Rahul, S. K., Abraham, A., Dusek, F., and Pappa, N. (2016). Teaching and Practicing Model Predictive Control. *IFAC-PapersOnLine*, vol. 49, pp. 34-39, July 2016.

[9] Jin, Z. L., Weng, J. S. and Hu, H. Y. (2007). Rollover stability of a vehicle during critical driving maneuvers. *Proceedings of the Institution of Machanical Engineers, Part D: Journal of Automobile Engineering*, vol. 221, no. 9, pp. 1041-1049, Sept. 2007.

[10] Caldwell, V. C., Dunlap, D. D. and Collins, G. E. (2010). Motion Planning for an Autonomous Underwater Vehicle via Sampling Based Model Predictive Control. *OCEANS 2010 MTS/IEEE SEATTLE*, Sept. 2010.

[11] Change, L., Seungho, L., Scott, V. and H. Eric Tseng. (2017). Path Planning for autonomous vehicle using model predictive control. *2017 IEEE Intelligent Vehicle Symposium (IV) Conference*, June 2017.

[12] Gwayi. I. and Tsoeu, M.S. (2018). Rollover Prevention and Path Following of Autonomous Vehicle using nonlinear Model Predictive Control. *2018 Open Innovation Conference (OI)*, pp. 13-18, 2018.

[13] Weiskircher, T. and Ayalew, B. Predictive ADAS: A predictive trajectory guidance scheme for advanced driver assistance in public traffic. *2015 European Control Conference (ECC)*, July 2015.

[14] Ford, J. and Thompson, J. (1969) Vehicle Rollover Dynamics Prediction by Mathematical Model. *SAE Technical Paper*, 1969.

[15] Thomas D. Gillespie. (1992). Fundamentals of Vehicle Dynamics. *Society of Automotive Engineers, Inc*, 1992.

[16] Guidelines on Maximum Weights and Dimensions of Mechanically Propelled Vehicles and Trailers, Including Maneuverability Criteria.

[17] Ginsberg, J. (1995). Advanced Engineering Dynamics. *Cambridge: Cambridge University Press*, 1995.

[18] M. Doumiati, A. Victorino, A. Charara and D. Lechner. (2009). Lateral load transfer and normal forces estimation for vehicle safety: experimental test. *Vehicle System Dynamics: International Journal of Vehicle Mechanics and Mobility*, Nov. 2009.

[19] Anake Umsrithong and Corina Sandu, (2010). A 3D Semi-Empirical On-Road Transient Tire Model. *SAE Technical Papers*, p 42-59, Dec. 2010.

[20] Yunta, J., Pozuelo, G.D., Diaz, V. and Olatunbosun, O. (2018). A Strain-Based Method to Detect Tires' Loss of Grip and Estimate Lateral Friction Coefficient from Experimental Data by Fuzzy Logic for Intelligent Tire Development. *Sensors*, vol. 18, n. 2, Feb. 2018.

[21] Bakker, E., Nyborg, L., and Pacejka, H. (1987). Tyre Modelling for Use in Vehicle Dynamics Studies. *SAE Technical Paper*, 1987.

[22] Rajamani, Rajesh. (2011). Vehicle Dynamics and Control, *Springer*, 2011.

[23] Paden, B., Cap, M., Yong, Z.S., Yershov, D. and Frazzoli, E. (2016). A Survey of Motion Planning and Control Techniques for Self-Driving Urban Vehicles. *IEEE Transactions on Intelligent Vehicles*, vol. 1, n. 1, pp. 33-35, June 2016.

[24] Honc, D., Sharma, K. R., Abraham, A., Dusek, F. and Pappa, N. (2016). Teaching and Practicing Model Predictive Control. *IFAC – Papers Online*, vol. 49, n. 6, pp. 34-9, 2016.

[25] Ding, B., Cychowski, T. M., Xi, Y., Cai, W. and Huang, B. (2012). Model Predictive Control. *Journal of Control Science and Engineering, Hindawi Publishing Corporation*, 2012.

[26] Wikipedia. (n.d.). Retrieved from

https://en.wikipedia.org/wiki/Model_predictive_control#Nonlinear_MPC

[27] Andersson J., Åkesson J. and Diehl M. (2012). CasADi: A Symbolic Package for Automatic Differentiation and Optimal Control. In: Forth S., Hovland P., Phipps E., Utke J., Walther A. (eds) Recent Advances in Algorithmic Differentiation. *Lecture Notes in Computational Science and Engineering*, *Springer*, July 2012.

[28] Andersson, A. E. J., Gillis, J., Horn, G., Rawlings, B. J. and Diehl, M. (2018). CasADi - A software framework for nonlinear optimization and optimal control. *Mathematical Programming Computation*, vol. 11, n. 1, pp. 1-36, March 2018.

[29] Seborg, Dale E. (2016). Process dynamics and control. *Hoboken, NJ: John Wiley & Sons, Inc.*, 2016.

[30] Chu, D., Ma, J. and Li, G. (2012). Active roll stability control for vehicle rollover prevention with combined dynamics modeling. *International Journal of Advancements in Computing Technology*, vol. 4, n. 8, pp. 26-35, May 2012.

[31] Lee, S., Yakub, F., Kasahara, M. and Mori, Y. (2013). Rollover prevention with predictive control of differential braking and rear wheel steering. *2013 6th IEEE Conference on Robotics, Automation and Mechatronics (RAM)*, Nov. 2013.

[32] Vehicle Stopping Distance and Time. (n.d.). Retrieved from

http://www.csgnetwork.com/stopdistinfo.html

[33] Rijswijk. (2018). PreScan, TASS International.

ABSTRACT

VEHICLE ROLLOVER STABILITY AND PATH PLANNING IN ADAS USING MODEL PREDICTIVE CONTROL

by

XINYUE ZHANG

May 2019

Advisor: Dr. Caisheng Wang

Co-Advisor: Dr. Chin-An Tan

Major: Electric-drive Vehicle Engineering

Advanced Driver Assistance Systems (ADAS) have been developed in recent years to significantly improve safety in driving and assist driver's response in extreme situations in which quick decisions and maneuvers are required. Common features of ADAS in modern vehicles include automatic emergency braking (AEB), lane keeping assistance (LKA), electric stability control (ESC), and adaptive cruise control (ACC). While these features are developed primarily based on sensor fusion, image processing and vehicle kinematics, the importance of vehicle dynamics must not be overlooked to ensure that the vehicle can follow the desired trajectory without inducing any instability. In many extreme situations such as object avoidance, fast maneuvering of vehicles with high center of gravity might result in rollover instability, an event with a high fatality rate. It is thus necessary to incorporate vehicle dynamics into ADAS to improve the robustness of the system in the path planning to avoid collision with other vehicles or objects and prevent vehicle

instability. The objectives of this thesis are to examine the efficacy of a vehicle dynamics model in ADAS to simulate rollover and to develop an active controller using Model Predictive Control (MPC) to manipulate the front-wheel steering and four-wheel differential braking forces, which are related to active steering as well as dynamic stability control for collision avoidance. The controller is designed using the model predictive control approach. A four degree-of-freedom vehicle model is simulated and tested in various scenarios. According to simulation results, the vehicle controller by the MPC controller can track the predicted path within error tolerance. The trajectories used in different simulation scenarios are generated by the MPC controller.

AUTOBIOGRAPHICAL STATEMENT

XINYUE ZHANG is a master student at Wayne State University major in Electric-drive Vehicle Engineering. She received her bachelor's degree in Mechanical Engineering from Zhejiang University of Technology, June 2018.